Clim Dyn (2013) 40:2825–2847
DOI 10.1007/s00382-012-1475-0

Analysis of the non-linearity in the pattern and time evolution of El Niño southern oscillation

Dietmar Dommenget · Tobias Bayr · Claudia Frauen

Received: 5 March 2012 / Accepted: 25 July 2012 / Published online: 9 August 2012

Abstract In this study the observed non-linearity in the spatial pattern and time evolution of El Niño Southern Oscillation (ENSO) events is analyzed. It is shown that ENSO skewness is not only a characteristic of the amplitude of events (El Niños being stronger than La Niñas) but also of the spatial pattern and time evolution. It is demonstrated that these non-linearities can be related to the non-linear response of the zonal winds to sea surface temperature (SST) anomalies. It is shown in observations as well as in coupled model simulations that significant differences in the spatial pattern between positive (El Niño) versus negative (La Niña) and strong versus weak events exist, which is mostly describing the difference between central and east Pacific events. Central Pacific events tend to be weak El Niño or strong La Niña events. In turn east Pacific events tend to be strong El Niño or weak La Niña events. A rotation of the two leading empirical orthogonal function modes illustrates that for both El Niño and La Niña extreme events are more likely than expected from a normal distribution. The Bjerknes feedbacks and time evolution of strong ENSO events in observations as well as in coupled model simulations also show strong asymmetries, with strong El Niños being forced more strongly by zonal wind than by thermocline depth anomalies and are followed by La Niña events. In turn strong La Niña events are preceded by El Niño events and are more strongly forced by thermocline depth anomalies than by wind anomalies. Further, the zonal wind response to sea surface temperature anomalies during strong El Niño events is stronger and shifted to the east relative to strong La Niña events, supporting the eastward shifted El Niño pattern and the asymmetric time evolution. Based on the simplified hybrid coupled RECHOZ model of ENSO it can be shown that the non-linear zonal wind response to SST anomalies causes the asymmetric forcings of ENSO events. This also implies that strong El Niños are mostly wind driven and less predictable and strong La Niñas are mostly thermocline depth driven and better predictable, which is demonstrated by a set of 100 perfect model forecast ensembles.

Keywords El Nino Southern Oscillation · El Nino Modoki · ENSO teleconnections · ENSO dynamics · Seasonal to interannual predictions · Tropical Pacific climate variability

D. Dommenget (✉) · C. Frauen
School of Mathematical Sciences, Monash University, Clayton, VIC, Australia
e-mail: dietmar.dommenget@monash.edu

T. Bayr
Helmholtz Centre for Ocean Research Kiel (GEOMAR), 24105 Kiel, Germany

1 Introduction

The El Niño Southern Oscillation (ENSO) mode can to first order be described by one standing sea surface temperature (SST) pattern whose amplitude increases or decreases over time (e.g. empirical orthogonal function (EOF) 1, see Fig. 1). However, it has also been noted that observed and simulated ENSO events can have different patterns, in particular it has been pointed out that El Niño events are different in pattern from La Niña events (e.g. Hoerling et al. 1997; Monahan 2001; Rodgers et al. 2004; Schopf and Burgman 2006; Sun and Yu 2009; Yu and Kim 2011; Takahashi et al. 2011; Choi et al. 2011). Further, it has been noted that the time evolutions of strong El Niño events are different from those of strong La Niña events (Larkin and Harrison 2002; Ohba and Ueda 2009;

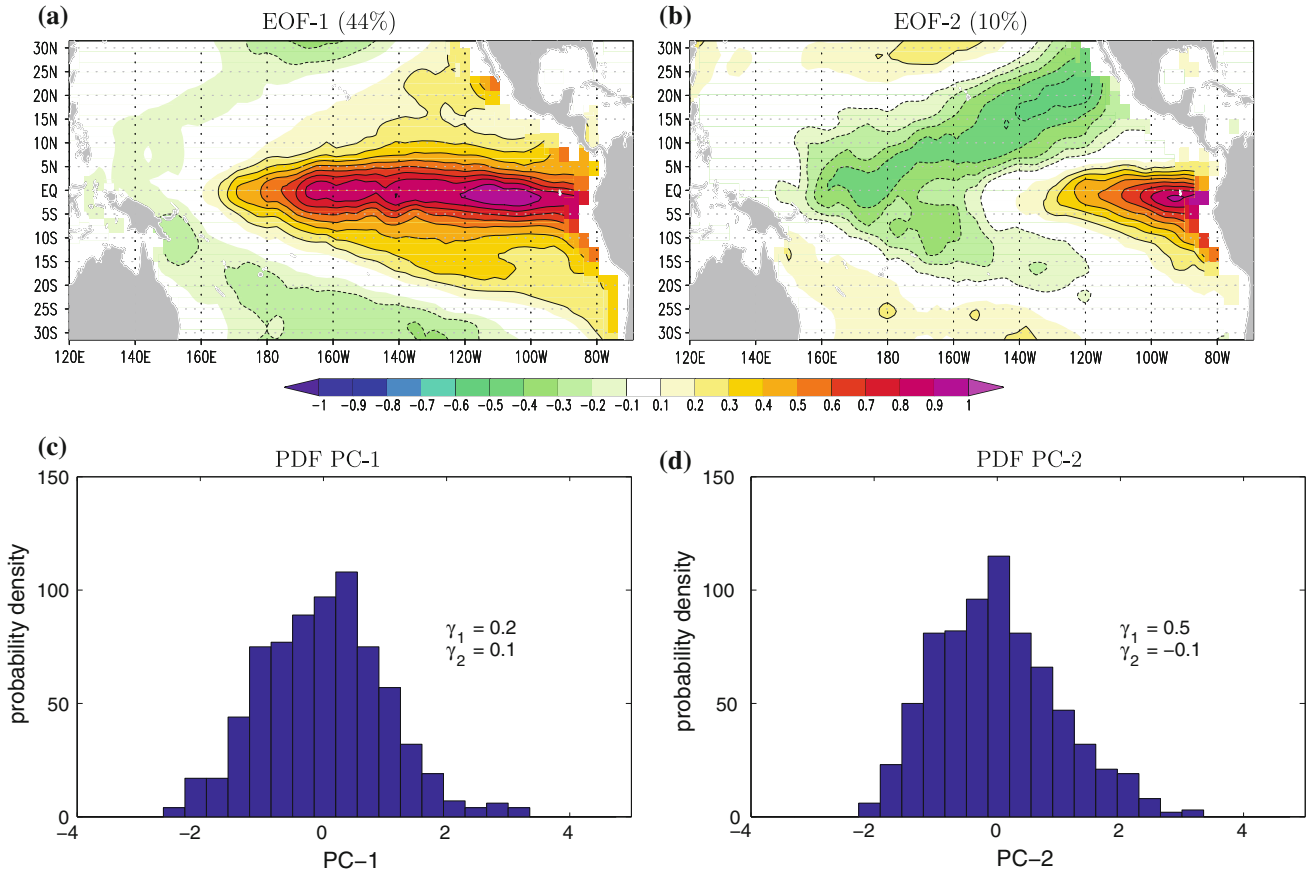

Fig. 1 **a** EOF-1 and **b** EOF-2 patterns of the HADISST linear detrended monthly mean SST anomalies from 1950 to 2010 are shown in the *upper panels*. The associated PC probability density distribution function of **c** PC-1 and **d** PC-2 with the distribution shape parameters skewness (γ_1) and kurtosis (γ_2) are shown in the *lower panels*

Okumura and Deser 2010). These differences in the shape of the patterns and the asymmetry in the time evolution represent a non-linearity of ENSO. The fact that non-linearities in the ENSO mode are important has in the literature mostly been noted in the context of the amplitude of El Niño or La Niña events, reflecting the skewness of the probability distribution of NINO3 SST anomalies. Processes that could cause non-linearities in the ENSO-mode include oceanic, biological and atmospheric processes. The later has been the focus of a series of recent publications (Kang and Kug 2002; Philip and van Oldenborgh 2009; Frauen and Dommenget 2010). The studies found that the skewness of NINO3 SST anomalies can be explained by the non-linear response of the zonal winds in the central Pacific to SST anomalies. The aim of the study presented here is to illustrate that the skewness of the probability distribution of ENSO events also reflects itself in the pattern shape and in the time evolution of ENSO events and that these non-linearities or asymmetries are at least partially caused by a non-linear response of the central Pacific zonal wind to SST anomalies.

The different shape of ENSO events has in recent years caught quite some attention, with several studies focusing on El Niño events that are centered in the central Pacific (e.g. Larkin and Harrison 2005; Ashok et al. 2007; Kao and Yu 2009; Yeh et al. 2009; Takahashi et al. 2011 or McPhaden et al. 2011). These type of events are named El Niño Modoki by Ashok et al. (2007). They argue that El Niño Modoki events are independent of the 'canonical El Niño' events, controlled by different dynamics. The analysis presented here aims to illustrate that these different ENSO types are at least partially related to non-linearities of the ENSO mode.

The article is organized as follows: In Sect. 2 we will present the observational data sets and model simulations used. In the first analysis Sect. 3, we will present the observed non-linearity in the ENSO event patterns and quantify it in terms of simplified indices. In Sect. 4 we analyze the non-linearities in the Bjerknes feedbacks and the time evolution of the ENSO events to explore the causes of the differences in the ENSO patterns. The observational evidences are then further backed up in Sect.

5 by state of the art coupled model simulations showing the same non-linearity characteristics. In Sect. 6 we will use the strongly simplified hybrid coupled model of Frauen and Dommenget (2010) to illustrate how the non-linearities in the feedbacks and time evolution relate to the non-linear response of the zonal wind to SST anomalies. The analysis part is completed with some discussion on how these non-linearities in the ENSO pattern relate to the different definitions of ENSO types (Sect. 7). Finally, we summarize and discuss the main findings of this study in Sect. 8.

2 Data and models

The analysis presented here is based on observed linear detrended SST anomalies for the period 1950–2010 taken from the HADISST data set (Rayner et al. 2003). Additional analysis with the ERSST data set (Smith et al. 2008) are done to support the results with the HADISST data set.

The observed sea level pressure (SLP) and 10 m zonal wind is taken from the NCEP reanalysis data from 1950 to 2008 (Kalnay et al. 1996). Since subsurface ocean observations are rare prior to the mid-1980s, the observed equatorial Pacific thermocline depths are estimated by the Max Planck Institute Ocean Model (MPI-OM) ocean general circulation model (Marsland et al. 2003) forced with the NCEP-reanalysis from 1948 to 2001. Data from this simulation was used also in previous studies of tropical coupled dynamics (e.g. Keenlyside and Latif 2007; Jansen et al. 2009).

The coupled general circulation model simulations analyzed in this study are taken from the CMIP3 database 20th century control simulations (Meehl et al. 2007). All models in the database that have a 20th century control simulation available are taken into account for this study. For all following analyses the 24 model simulations have been interpolated onto a regular 2.5° × 2.5° global grid.

The hybrid coupled RECHOZ model is a 500 years long simulation with simplified linear ocean dynamics in the tropical Pacific, a single column ocean model outside the tropical Pacific and a fully complex atmosphere model (ECHAM5), see Frauen and Dommenget (2010) for details. The RECHOZ model is also used for a sensitivity study in which the tropical SST variability outside the tropical Pacific is removed.

3 Observed El Niño pattern non-linearity

The non-linearity of the ENSO pattern can in a first attempt be summarized by splitting the SST anomalies into four categories, defined by two characteristics of NINO3.4 SST anomalies: the sign and the strength. The average patterns for each of the four categories are shown in Fig. 2. Each of these four mean composite patterns has been normalized by the mean NINO3.4 SST anomalies of each composite, which allows comparing the relative shape of each pattern against the shapes of the other patterns. Subsequently, the composites for negative events have been presented with revised signs for better comparison with the patterns of positive events. Note, that not all data is represented by the four categories, as data points with the SST anomaly of NINO3.4 near zero are not considered in any of the four categories. Several combinations of the differences between the mean patterns are shown as well to highlight the differences between positive versus negative and strong versus weak events. The following mean features should be pointed out here:

- Following a students T test assuming every 12 months are independent, the eastern pole along the equator is significantly (95 % confidence level) different from the zero null hypothesis in all four difference patterns. The most significant differences are seen in Fig. 2c with all of the contoured regions passing the 95 % confidence level and the least significant differences are seen in Fig. 2h with only the eastern pole around the equator passing the 95 % confidence level.
- Strong El Niño events are significantly shifted to the east and are more closely confined to the equator than strong La Niña events.
- Almost the exact opposite is true for weak events: weak El Niño events are significantly shifted to the west and have larger meridional extend than weak La Niña events.
- The difference between strong and weak El Niño events is almost the same as the difference between strong El Niño and strong La Niña events.
- The same holds for the difference between strong and weak La Niña events.
- Subsequently, the mean pattern of a strong El Niño event is similar to the mean pattern of a weak La Niña event with the opposite sign, and the mean pattern of a weak El Niño event is similar to the mean pattern of a strong La Niña event with the opposite sign.
- All difference patterns have basically the same equatorial shifts and all strongly project onto the pattern of EOF-2 (see Figs. 1b or 2i and pattern correlation values in headings of Fig. 2).

A similar selection of ENSO events has been made by Sun and Yu (2009), Yu and Kim (2011) and Choi et al. (2011). Those results largely agree with those presented here, but their discussion focuses on decadal ENSO modulations, while here we like to focus on the non-linearity of the interannual ENSO variability.

The significant differences in the ENSO event types (e.g. strength or sign) basically mean that they cannot be

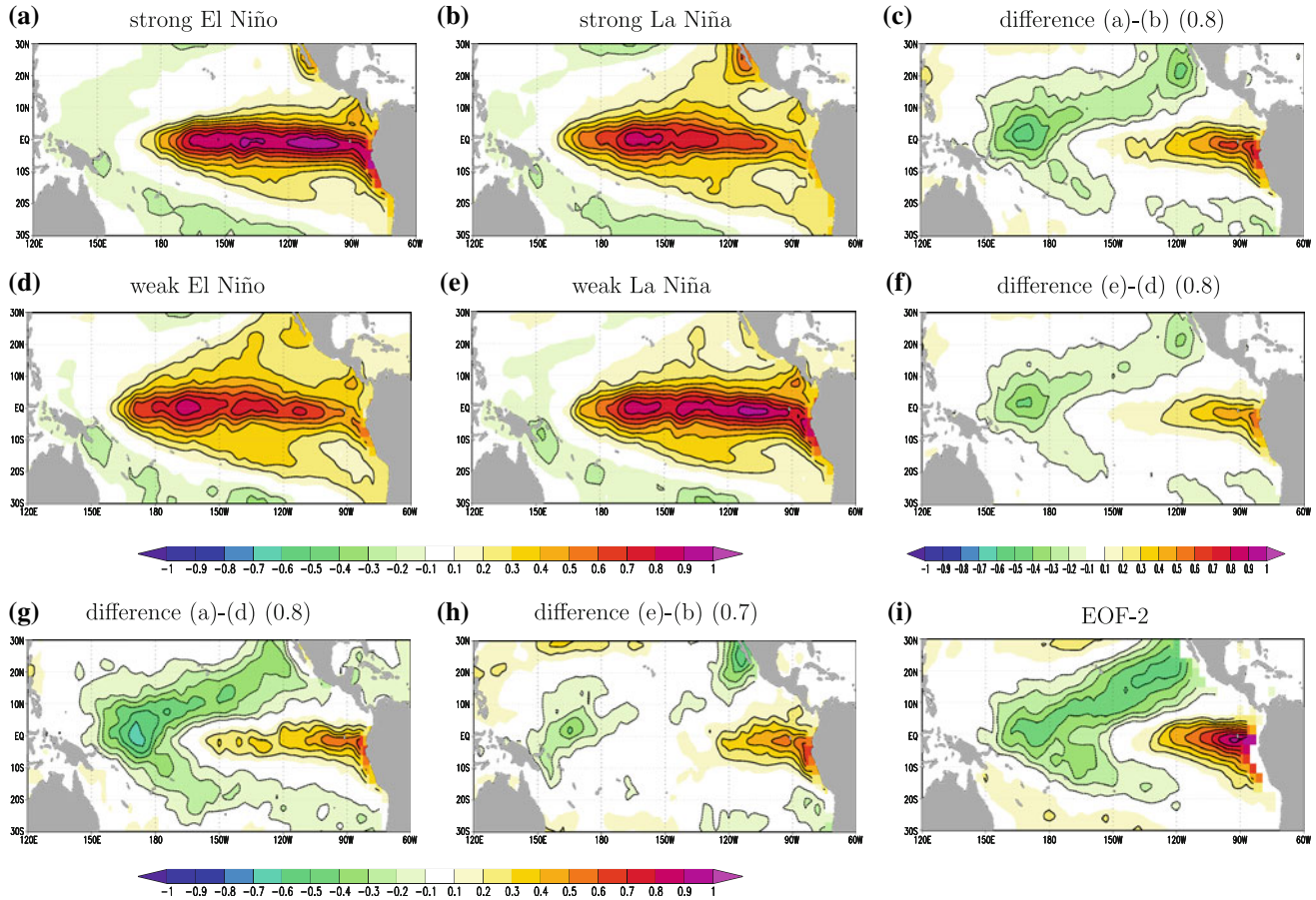

Fig. 2 Composites of HADISST linear detrended monthly mean SST anomalies from 1950 to 2010 based on NINO3.4 SST anomalies. **a** for all data with NINO3.4 SST anomalies >1°K, **b** with NINO3.4 SST anomalies less than −1°K, **d** with NINO3.4 SST anomalies >0.5°K and <1°K and **e** with NINO3.4 SST anomalies less than −0.5°K and greater than −1°K. All Composites are normalized by their mean NINO3.4 SST anomalies. Thus **b** and **e** are shown with the reversed sign of the mean SSTs, as the mean NINO3.4 SST anomalies of these composites is negative. **c** The difference between (**a**) and (**b**), **f** the difference between (**e**) and (**d**), **g** the difference between (**a**) and (**d**) and **h** the difference between (**e**) and (**b**). Panel **i** shows the EOF-2 pattern of Fig. 1b for comparison. The headings in **c**, **f**, **g** and **h** show the difference pattern correlation values with the EOF-2 pattern. Units are in K/K (in NINO3.4 region) for (**a**)–(**h**) and non-dimensional for (**i**)

described completely by the evolution of one pattern (e.g. EOF-1). A strong El Niño event, for instance, is a superposition of the EOF-1 pattern plus the EOF-2 pattern and a strong La Niña event is a superposition of the EOF-1 pattern with negative sign and the EOF-2 pattern with positive sign. Thus, the EOF-2 has a non-linear co-variability with the EOF-1: whenever the EOF-1 is in an extreme phase (strong El Niño or strong La Niña) then EOF-2 is positive. This behavior can be seen in the time series of PC-1 and PC-2, see Fig. 3. All major strong El Niño events (e.g. years 1973, 1983 or 1997) have also positive PC-2 values, mostly with relatively strong magnitudes. The same holds for all major strong La Niña events (e.g. years 1974, 1989 or 1999). In turn the PC-2 tends to have negative values when the PC-1 is close to neutral values ($-1 <$ PC-1 < 1). To quantify this we can build composites of the six strongest El Niño events and the six strongest La Niña events and look at the time evolution of the composite mean values of PC-1 and PC-2 relative to the December of the events, see Fig. 3b and c. We can quite clearly see that both PC-1 and PC-2 peak during strong El Niño events. This can also be seen for strong La Niña events, but we can further notice that the strong La Niña events are preceded by El Niño events about a year earlier, which will be discussed further in Sect. 4.

This non-linear relation between the PC-1 and PC-2 can best be illustrated by a scatter plot of the time series of PC-1 versus that of PC-2; see Fig. 4a. If we assume that the EOF-1 and EOF-2 modes represent independent modes of variability (as often done in the interpretation of EOF-modes; e.g. Ashok et al. (2007)) with near normal distributions, then the scatter plot should be a circular shape cluster that peaks at the origin of the coordinate system. However, we can clearly see a skewed distribution. For

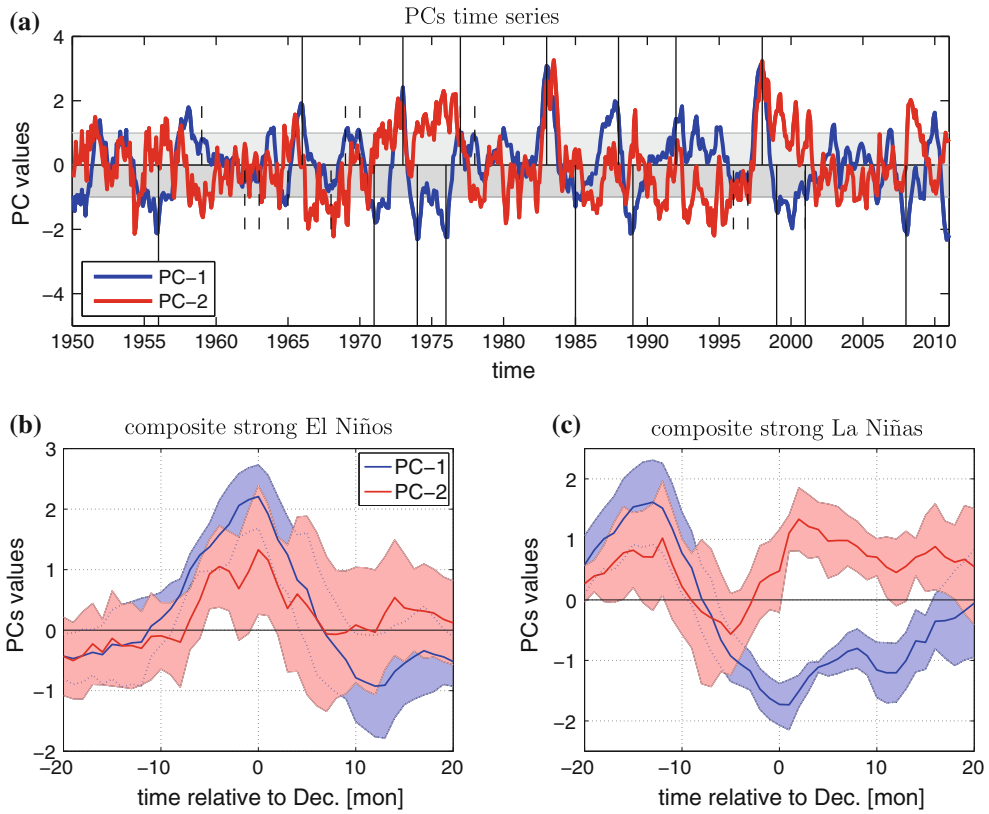

Fig. 3 **a** Time series of PC-1 (*blue*) and PC-2 (*red*). The *shaded areas* mark the ±1 intervals, which roughly matches the composites selection criteria for Fig. 2. The *vertical lines* in (**a**) mark the events used in Figs. 6 and 7. The mean lag/lead time evolution of the PC-1 and PC-2 time series for (**b**) composite mean time evolution for the 6 strongest El Niño events (1966, 1973, 1983, 1988, 1992 and 1998) and **c** the same for the 6 strongest La Niña events (1955, 1971, 1974, 1989, 1999 and 2008) are shown. The *shaded areas* around the PCs mark the 90 % confidence interval. The x-axis values refer to the month relative to December of each ENSO event

extreme values of PC-1 PC-2 tends to be positive and for PC-1 near zero PC-2 tends to be negative, which is consistent with the above discussion of the non-linear pattern and time series behavior. This non-linear relation between PC-1 and PC-2 can be relatively well modeled by a quadratic relationship:

$$\mathrm{PC2}_{\mathrm{non-linear}}(t) = r \cdot (\mathrm{PC1}(t))^2 \quad (1)$$

A fit of PC-2 to this model is shown in Fig. 4a. The PC-1 time series correlates with this non-linear model of PC-2 relatively well (correlation 0.51) and is clearly significantly different from the null hypothesis of zero correlation assuming a Students T test with 60 (each year) independent values (resulting t value $= 4.6$ corresponding to the 99.999 % value of the distribution). This quadratic relationship basically describes the results of Fig. 2, where we found that the difference between strong events of opposing signs is exactly the opposite of those of the weak events and the difference between strong and weak El Niño events is exactly the opposite to those of the La Niña events. PC-2 is positive if PC-1 takes large absolute values and it is negative if PC-1 takes small absolute values. The superposition of PC-1 and PC-2 then gives the effect of shifted peaks between changes of sign or changes in magnitude.

We can test if this non-linear relationship between PC-1 and PC-2 can account for the non-linearity seen in the ENSO event composites in Fig. 2 by excluding this non-linear relationship from the data. To do so, we reconstruct the SST variability with the 20 leading EOF-modes, but exclude the non-linear part of PC-2, $\mathrm{PC2}_{\mathrm{non\text{-}linear}}$, from the PC-2 time series, resulting into a residual PC-2 time series, $\mathrm{PC2}_{\mathrm{residual}}$, defined as:

$$\mathrm{PC2}_{\mathrm{residual}}(t) = \mathrm{PC2}(t) - \mathrm{PC2}_{\mathrm{non-linear}}(t) \quad (2)$$

If we apply the composite analysis of Fig. 2 to the reconstructed data, using the $\mathrm{PC2}_{\mathrm{residual}}$, we find the mean patterns shown in Fig. 5. We now see that all four mean patterns are quite similar and the difference patterns are mostly insignificant, indicating that the non-linear relationship between PC-1 and PC-2, as formulated in Eq. (1), does indeed describe the non-linear patterns of ENSO events relatively well and that higher order EOF-modes are to first order not needed to describe this phenomenon.

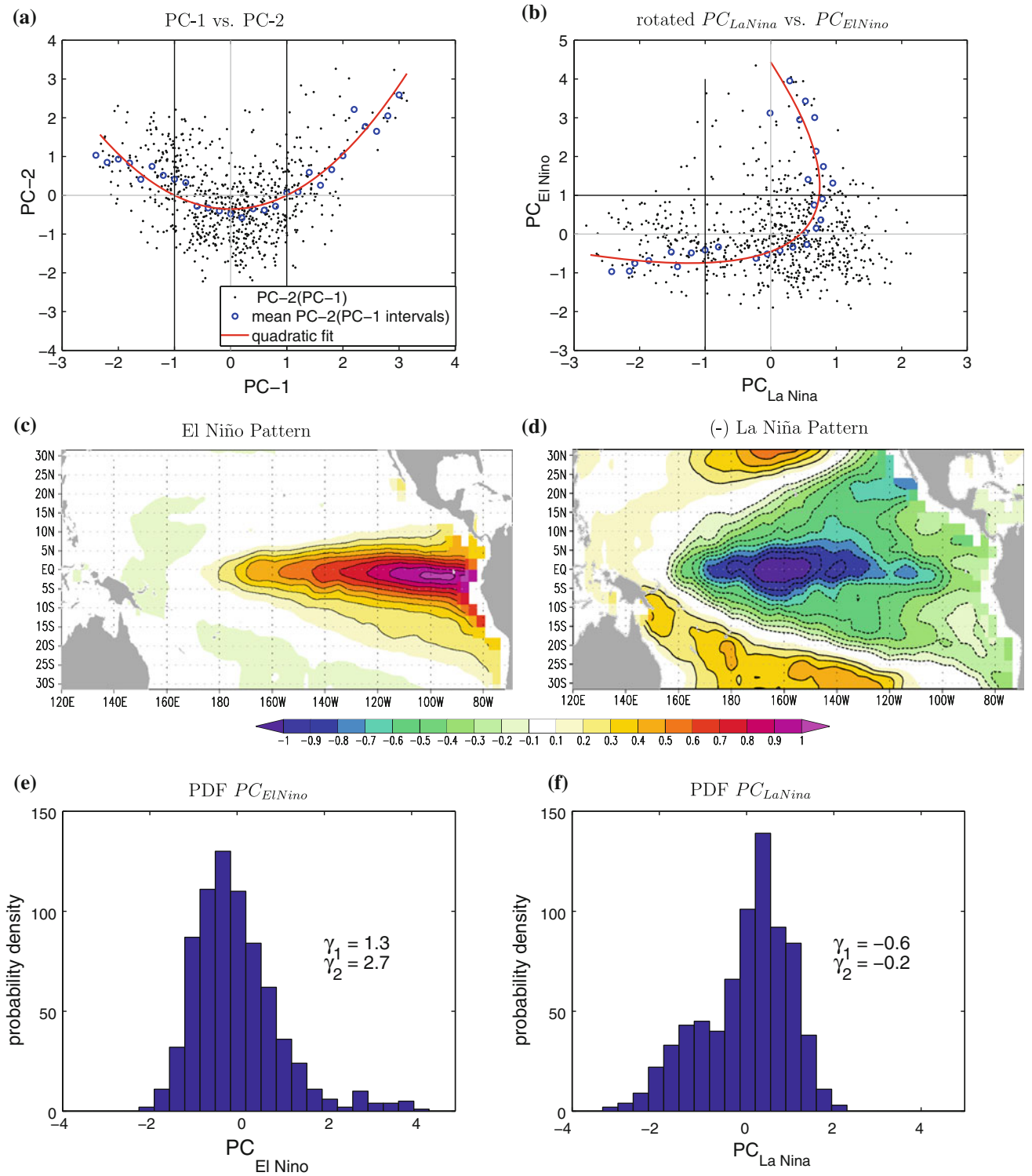

Fig. 4 **a** Scatter plot of tropical Pacific SST PC-1 and PC-2 data pairs (*black dots*) for each linear detrended monthly mean SST anomaly from 1950 to 2010 corresponding to the EOFs of Fig. 1. In addition the mean PC-2 values for 0.2 intervals of PC-1 are shown (*blue open circles*). The non-linear model of PC-2 as function of PC-1 [Eq. (1)] is marked by a *red line*. **b** A counter clockwise 45° rotation of (**a**), defining the new rotated axes $PC_{El\text{-}Niño}$ and $PC_{La\text{-}Niña}$. **c** The pattern corresponding to the rotated $PC_{El\text{-}Niño}$ and **d** the pattern corresponding to the rotated $PC_{La\text{-}Niña}$. **e** and **f** are as in Fig. 1c and d, but for **e** $PC_{El\text{-}Niño}$ and **f** $PC_{La\text{-}Niña}$

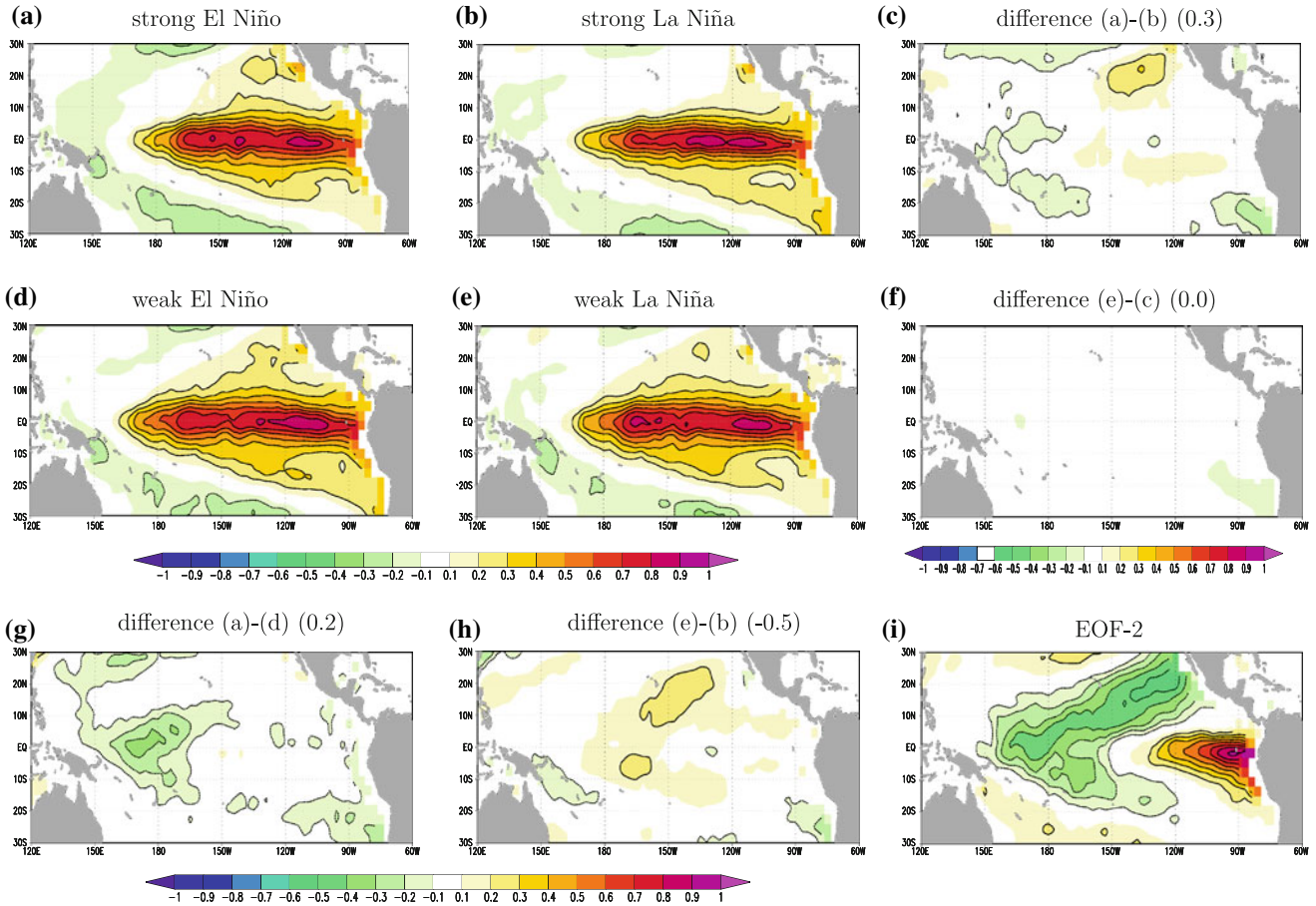

Fig. 5 Composites of HADISST SST anomalies as Fig. 2, but for the data reconstructed with the 20 leading EOF-modes and using $PC2_{residual}$ [see Eq. (2)] instead of PC-2, thus excluding the non-linear interaction between the EOF-1 and EOF-2 modes

The distribution of data points in Fig. 4a mainly scatters around the non-linear function $PC2_{non\text{-}linear}$. It therefore seems reasonable to select ENSO events relative to $PC2_{non\text{-}linear}$ (e.g. strong El Niño events are at the right end of the curve). However, we started the analysis of the spatial pattern non-linearity by selecting ENSO events by NINO3.4 SST anomaly values (Fig. 2). The NINO3.4 SST index is basically the same as the PC-1 (see also Takahashi et al. (2011)) and thus follows the PC-1 axis. Therefore, a selection of positive or negative, strong or weak ENSO events was done by splitting the distribution along constant lines of the PC-1 axis in Fig. 4a (e.g. strong El Niño events in Fig. 2a are essentially all values with PC-1 > 1.0), which cuts through the line of $PC2_{non\text{-}linear}$ at a non-orthogonal angle. This is not the optimal way to select the events, as the distribution is relatively wide in this direction. If we rotate the distribution of Fig. 4a by 45° counter clockwise we find a presentation in which we can select strong El Niño (>1 on the new y-axis) and strong La Niña events (less than -1 on the new x-axis) with lines of constant values of the new main axes and roughly orthogonal to the $PC2_{non\text{-}linear}$ curve, see Fig. 4b. The new rotated axes $PC_{El\text{-}Niño}$ and $PC_{La\text{-}Niña}$ are an orthogonal rotation of the PC-1 and PC-2:

$$\begin{aligned} PC_{El-Ni\ no} &= (PC1 + PC2)/\sqrt{2}; \\ PC_{La-Ni\ na} &= (PC1 - PC2)/\sqrt{2} \end{aligned} \tag{3}$$

Takahashi et al. (2011) defined the same rotation base on similar arguments. The patterns corresponding to the $PC_{El\text{-}Niño}$ and $PC_{La\text{-}Niña}$ are shown in Fig. 4c and d. Due to the 45° rotation both modes explain equal amounts (27 %) of the total variance. The El Niño pattern is clearly shifted to the east and more confined to the equator than EOF-1, which is consistent with the discussion of the composite non-linearity in Fig. 2. In turn the La Niña pattern is clearly shifted to the west and much wider in its meridional extent than EOF-1. These patterns basically present the non-linear spatial structure of ENSO events in an optimal way.

It is interesting to compare the probability distributions of $PC_{El\text{-}Niño}$ and $PC_{La\text{-}Niña}$ with those of PC-1 and PC-2, see

Fig. 4e and f and Fig. 1c and d. The following points should be noted here:

- The PC-1 and PC-2 are both much closer to a normal distribution than $PC_{El\text{-}Niño}$ and $PC_{La\text{-}Niña}$, which is illustrated by the skewness and kurtosis values.
- The central limit theorem suggests that distributions that follow a normal distribution are a sum of many processes adding up to the distribution. This in turn would suggest that the EOF-modes are more likely to present some superposition of several processes than the $PC_{El\text{-}Niño}$ and $PC_{La\text{-}Niña}$ modes as they are more normally distributed. The characteristic that EOF-modes tend to be super positions of many 'physical' modes has been discussed in some more detail in Dommenget and Latif (2002).
- In turn the stronger non-normality present in the distributions of the $PC_{El\text{-}Niño}$ and $PC_{La\text{-}Niña}$ modes indicates that these modes are more likely to focus on low-order specific physical processes than the EOF-modes.
- The skewness and kurtosis of the $PC_{El\text{-}Niño}$ is larger than that of the EOF-1 and NINO3 SST anomalies. Thus the $PC_{El\text{-}Niño}$ index identifies much more extreme positive El Niño events, than the PC-1 and NINO3 SST indices.
- The $PC_{La\text{-}Niña}$ has a strong negative skewness, suggesting a strong non-linearity towards extreme La Niña events that is not reflected in any of the conventional large-scale indices of ENSO.

In summary, we find that the non-linear spatial pattern of ENSO events is relatively well described by the rotation of the first two PCs into the $PC_{El\text{-}Niño}$ and $PC_{La\text{-}Niña}$ modes. This presentation gives a very good separation of extreme El Niño or La Niña events from moderate events or neutral conditions. For the subsequent analysis we will in most cases use the two rotated modes to define extreme events, as they are the dynamically better presentations. Note that weak events cannot be selected by the rotated modes very well, as they would be mixed up between the $PC_{El\text{-}Niño}$ and $PC_{La\text{-}Niña}$ modes (compare Fig. 4 a and b). However, most of the following composites will only show minor changes if the selections are based on NINO3.4 SST or PC-1 indices.

4 Observed feedbacks

In the following analysis we want to explore the time evolution and feedbacks related to extreme ENSO events to gain some understanding of what causes the non-linearities in the events. The main feedbacks associated with ENSO are the Bjerknes feedbacks, which describe interactions between zonal wind, SST and the depth of the thermocline. Since the feedbacks control the evolution of the events it is instructive to analyze the lag-lead time evolution of event composites.

As a starting point we analyze the lag-lead time evolution of the equatorial Pacific SST for strong and weak El Niño and La Niña events, see Fig. 6. A few characteristics can be noted here:

- First of all near lag 0 (in Fig. 6a–c) we find the same characteristic east-west shift between strong El Niño and La Niña events as in Fig. 2. Thus at lag zero this figure is basically another way of presenting the same spatial asymmetry as in Fig. 2.
- The same holds for the east-west shift of the weak events, but just with the opposite sign. Note that the weak events are selected by PC-1, as the rotated PCs are not useful for selecting weak events. See discussion above.
- The most interesting aspect in the lag-lead time evolution of the strong events is the significant non-linearity at about 1 year before and after the event (December). The La Niña events at around 1 year after strong El Niño events tend to be stronger than those preceding. Whereas in turn strong La Niña events are not followed by El Niño events 1 year later. Further, a strong La Niña event is preceded by a significant El Niño anomaly in the eastern equatorial Pacific, whereas strong El Niño events do not have such a significant preceding La Niña anomaly. The time evolution difference in the NINO3.4 region between 5–10 mon before and after lag 0 is statistically very significant ($\gg$99 % value of the t test distribution). This was also indicated in the PCs mean composite time evolutions shown in Fig. 3b and c. The asymmetric time evolution described here is in good agreement with similar findings of Ohba and Ueda (2009) and Okumura and Deser (2010).
- The opposite time evolution we find for the weak events. Here a weak La Niña event is followed by a significant El Niño anomaly a year later, whereas in turn weak El Niño events are not followed by La Niña events.

In summary this lag-lead time evolution of the ENSO events suggests that the driving mechanisms for El Niño and La Niña events are different. The fact that strong La Niña events tend to follow an El Niño event, could suggest that the strong La Niña events are triggered partially by the ocean state set by the preceding El Niño event. In turn no such preset ocean state may exist for strong El Niño events, which in turn would suggest that strong El Niño events might be forced by random atmospheric forcings that may be unpredictable. The opposite may hold for weak events.

Before we look at the elements of the Bjerknes feedbacks we first examine the atmospheric evolution during

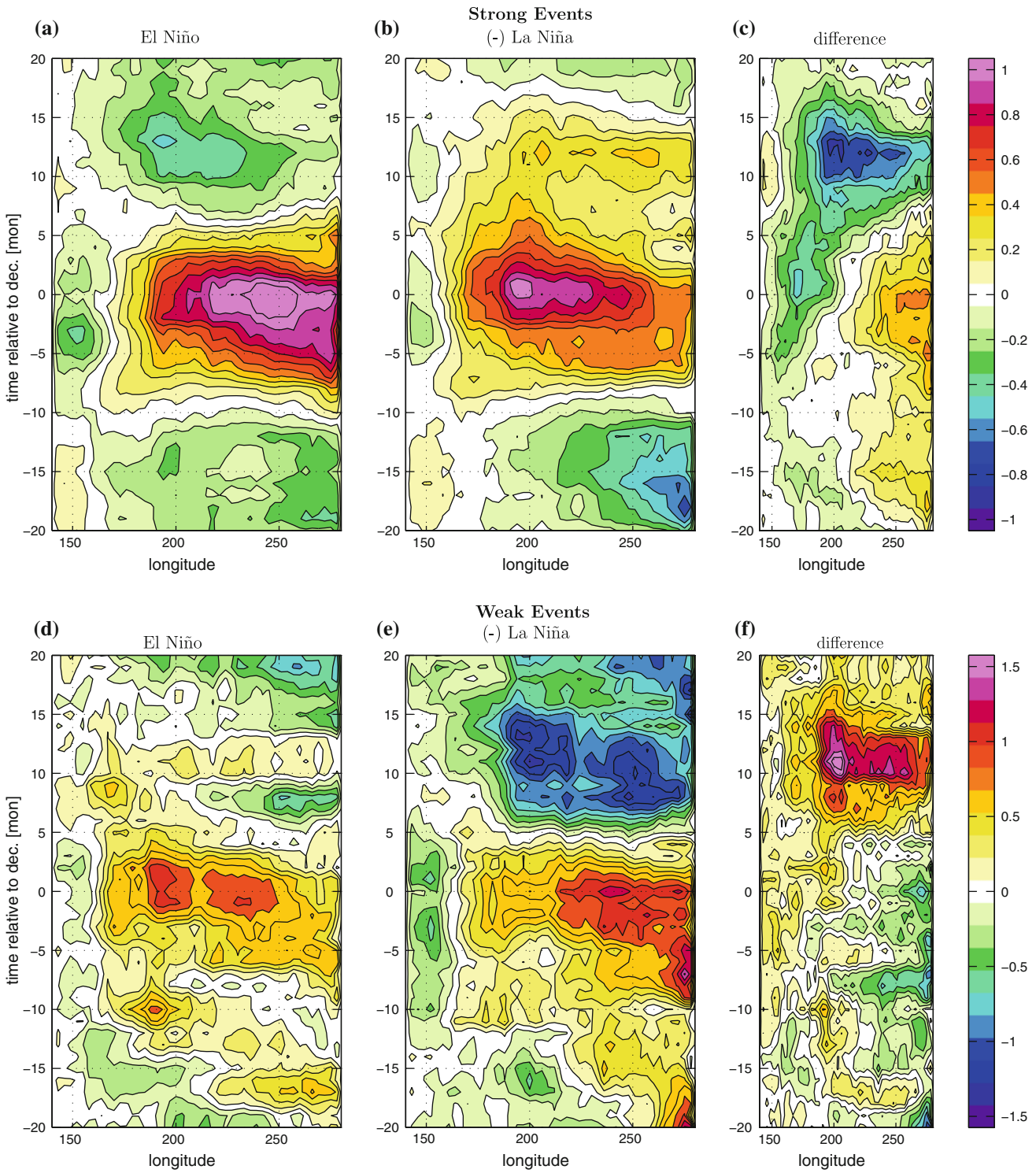

Fig. 6 Composite Hoevmoeller diagrams of the equatorial (averaged between 5°S and 5°N) Pacific SST anomalies for **a** strong ($PC_{El\text{-}Niño} > 1.0$ in December) and **d** weak ($1.0 > PC\text{-}1 > 0.5$ in December) El Niño events and **b** strong ($PC_{La\text{-}Niña} < -1.0$ in December) and **d** weak $-1.0 < PC\text{-}1 < -0.5$ in December) La Niña events are shown. All Composites are normalized by their mean NINO3.4 SST anomalies in the Decembers that passed the selection criteria. Thus **b** and **e** are shown with the reversed sign of the mean SST anomalies, as the mean December NINO3.4 SST anomalies of these composites is negative. **c** The difference between (**a**) and (**b**) and **f** the difference between (**d**) and (**e**). The y-axis values refer to the month relative to the Decembers that passed the selection criteria for each ENSO composite. Units are in K/K (in NINO3.4 region)

strong events. The mean sea level pressure (SLP) is, to first order, a good estimator of the atmospheric evolution during strong ENSO events, see Fig. 7a–c. We can roughly see that the non-linearities in the SLP composites follow the main pattern of the SST non-linearities: The low pressure is shifted to the east roughly in line with the SST shift and the strong El Niño events are followed by a positive SLP anomaly about a year later, again in line with the SST evolution. Further we find that the SLP anomalies preceding strong El Niño events for a few months are stronger in amplitude than those of the strong La Niña events, again being consistent with the idea that the strong El Niño events may have been forced more strongly by atmospheric forcings than strong La Niña events.

More important for the understanding of the ENSO forcing is the zonal wind relation to SST, which is one element in the Bjerknes feedbacks. The zonal wind composites again show some significant non-linearities, see Fig. 7d–f. The following should be noted here:

- At around lag zero we find an east-west shift, by about 20°, in the same direction as the SST peak shifts. During strong El Niño events the westerly zonal wind anomalies are shifted to the east and are more pronounced over the whole of the equatorial Pacific east of the dateline. This basic structure of observed non-linearity in the zonal winds has also been described in Kang and Kug (2002) and Ohba and Ueda (2009).
- As in the SST and SLP evolution we also find that the zonal wind anomalies prior to the peak of strong El Niño events are stronger (per NINO3.4 SST anomaly) than in the strong La Niña events. In particular around the dateline and west of it. Indeed the peak of the zonal wind response is about 2 months earlier.
- Again the zonal winds show a reversed anomaly about a year after strong El Niño events in line with the SST anomalies, indicating a change to La Niña conditions after strong El Niño events.

While the zonal winds show a clear non-linearity between strong El Niño and La Niña events, we cannot yet conclude whether the zonal winds are a forcing or response to the SST. Thus it is unclear whether the non-linearity in the zonal winds is a response to the different SST patterns or whether the zonal winds cause the differences in the SST patterns. However, studies of Zhang and McPhaden (2006, 2010) give some support for the idea that the shifts in the zonal wind response would support the shifts in the SST patterns. They find that the SST in the eastern equatorial Pacific is sensitive to the local winds as well, with weakening of the zonal winds leading to warming of the SST, thus supporting the eastward shift during strong El Niño events. Some indications about cause and response will also be discussed later in the analysis of the simplified model simulations (Sect. 6), but for now we focus on presenting the non-linearities in the observed Bjerknes feedbacks.

The second element of the Bjerknes feedback is the thermocline depth sensitivity to zonal wind; see Fig. 7g–i. Note that unlike the previous composites the composites of thermocline depth anomalies are normalized by the mean zonal wind anomalies in the central Pacific (160°E–120°W) and not by the NINO3.4 SST anomalies, as we are interested in the sensitivity of thermocline depth to zonal wind, not SST. Some important non-linearities can be noted here:

- As for the zonal wind, we find a west to east shift in the thermocline anomalies by about 20°, which is however much further to the eastern side of the Pacific than in the zonal wind, as this is the region with the peak in the thermocline response.
- Also in line with the previous findings we find some indication of a change in sign in the thermocline anomalies following about 1 year after a strong El Niño event. Again indicating La Niña conditions following the strong El Niño events.
- In contrast to the SLP and zonal wind response, which are weaker for strong La Niña compared to strong El Niño events, we now find a weak indication of a stronger thermocline depth anomaly for strong La Niña events than for strong El Niño events. Averaged over the whole equation Pacific the thermocline depth anomalies preceding the strong La Niña events by about up to a year are more pronounced than for strong El Niño events. This result is mostly consistent with a similar finding by Ohba and Ueda (2009) using the SODA ocean reanalysis data for the period 1954–2004 (Carton et al. 2000).

In summary, we find some indications that the zonal winds preceding strong El Niño events are stronger than during strong La Niña events. Further, we find some weak indications that the thermocline response to zonal winds in strong La Niña events is stronger than in strong El Niño events. Both findings are consistent with the idea that strong La Niña events are more strongly forced by the ocean state than strong El Niño events, which are more strongly forced by the atmosphere.

5 CMIP3 model simulations

The analysis of observations is limited in quantity and quality. Some of the above results are only marginal significant and model simulations can therefore provide additional independent verifications. Further, the understanding of the processes involved in complex interactions

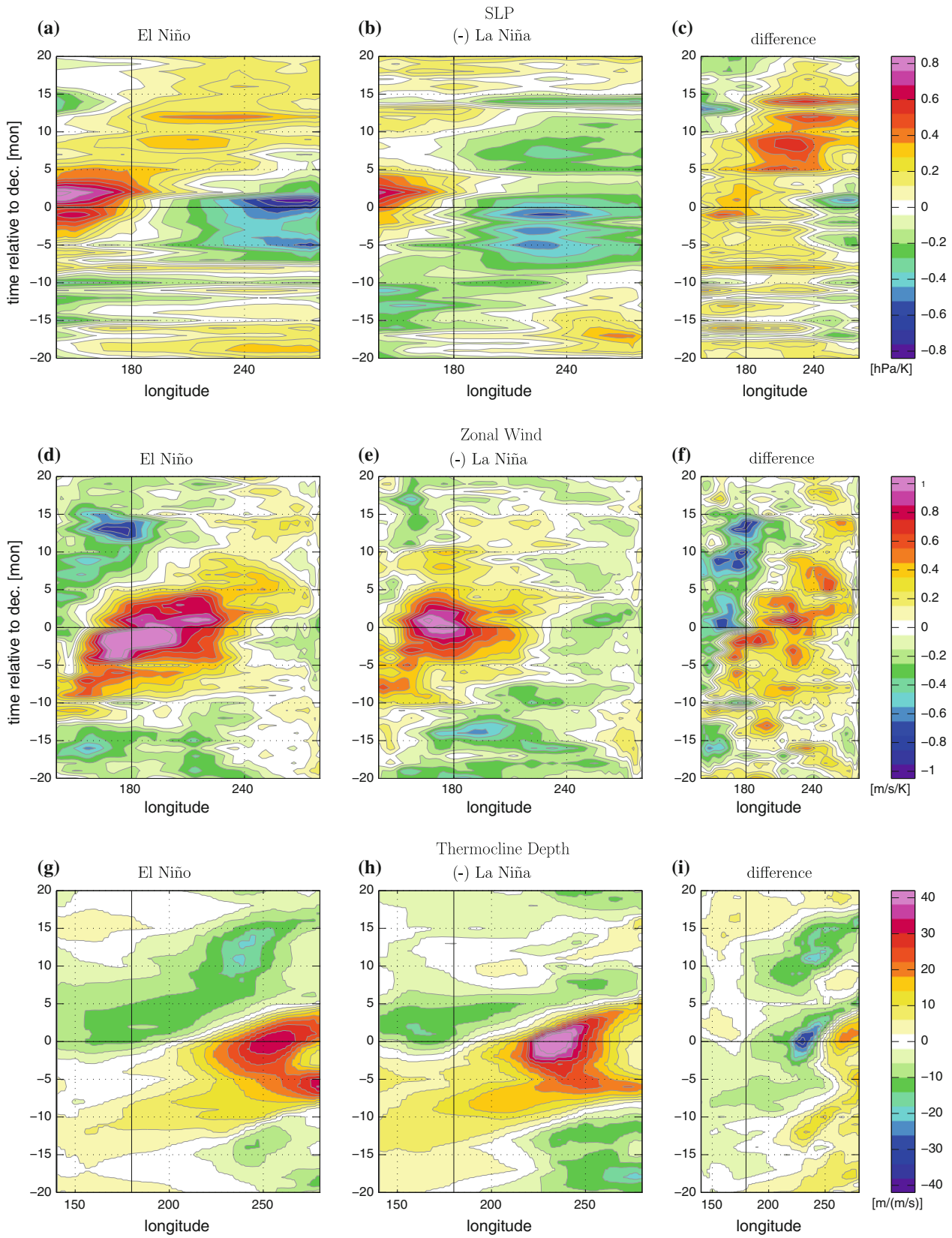

Fig. 7 Composite Hoevmoeller diagrams of the equatorial Pacific as in Fig. 6a–c, but for **a–c** SLP anomalies and **d–f** 10 m zonal wind anomalies from NCEP reanalysis and for **g–i** thermocline depth anomalies from the MPI-OM reanalysis. The thermocline depth composites are normalized by the mean zonal wind anomalies in the central Pacific (160°E–120°W) and not by the NINO3.4 SST anomalies

of ENSO is much easier achieved with model simulations as elements of the models can be taken apart. However, it has to be noted that the state of the art coupled general circulation models (CGCMs) are far from being perfect in simulating ENSO. Most CGCMs are quite limited in their skills of simulating main aspects of the ENSO mode. In particular the non-linear aspects of ENSO (e.g. skewness and kurtosis) are quite badly represented in most climate models (e.g. An et al. 2005 or van Oldenborgh et al. 2005). Indeed, most CMIP3 models are not capable of simulating the positive skewness of ENSO (e.g. NINO3 SST index). Therefore it seems likely that most CMIP3 models will also have problems in simulating the observed non-linear ENSO pattern evolutions that we have described above.

In order to quantify to what extent the CMIP3 models can simulate the asymmetry between El Niño and La Niña pattern and time evolution we defined two indices based on the composite differences along the equator, Δ_{eq}, and in the time evolution, Δ_{time}. The index Δ_{eq} is defined as the difference between the eastern equatorial Pacific (220°E–280°E/5°S–5°N) and the western equatorial Pacific (140°E–200°E/5°S–5°N) in the normalized composite difference as shown in Fig. 2c and the index Δ_{time} is defined as the difference between the mean NINO3.4 SST anomalies for lead times of 20–10 months minus mean NINO3.4 SST anomalies for lag times of 10–20 months as shown in the normalized composite difference Fig. 6c. The events are selected by the NINO3.4 index instead of values of the rotated PCs, as these are not defined for all the models. For the observations we used the 1 K in the NINO3.4 index for selection of strong events in Fig. 2, which corresponds to about 1.25 standard deviations of NINO3.4. Since the models standard deviations of NINO3.4 index are very different in the different models we also use 1.25 standard deviations of NINO3.4 of each model as a threshold instead of the 1 K threshold.

For the two observational data sets Δ_{eq}, is about 0.5 and Δ_{time} about 0.4 (both indices in [K] per [K] in the NINO3.4 index). In Fig. 8 we plotted the values for all 24 CMIP3 models in the 20th century simulations and the observations. We see that for most models the Δ_{eq} value fluctuates around zero, with 8 models even showing negative signs in Δ_{eq}, indicating strong El Niño events with larger amplitudes further to the west compared to strong La Niña events. The asymmetry in the time evolution is better represented in the models, with most models showing the same behavior (La Niñas following strong El Niños or El Niños preceding strong La Niñas). Overall the distribution of the models tends into the direction of the observed asymmetries, but only 4 models (GFDL 2.0, GFDL 2.1, IPSL and the MPI) are simulating both asymmetries relatively well. Yu and Kim (2011) did a similar selection of the CMIP3 models (excluding the MPI model) based on differences along the equator only. They additionally selected the MIUB and CNRM models, which in our selection either did not pass the Δ_{time} criteria (MIUB) or were too small in the Δ_{eq} criteria (CNRM). The CNRM model, however, does show all of the features that we discussed for the observations and the selected models below. Ohba et al. (2010) also did analysis of the asymmetric time evolution of the CMIP3 models. They come to similar conclusions and their analysis also showed that the GFDL 2.0, GFDL 2.1, IPSL and the MPI show some asymmetric time evolution consistent with the observations.

The fact that most models fail our selection criteria first of all indicates that most models are not capable of simulating the ENSO pattern and time evolution non-linearity realistically. However, the set of 4 models seems to have

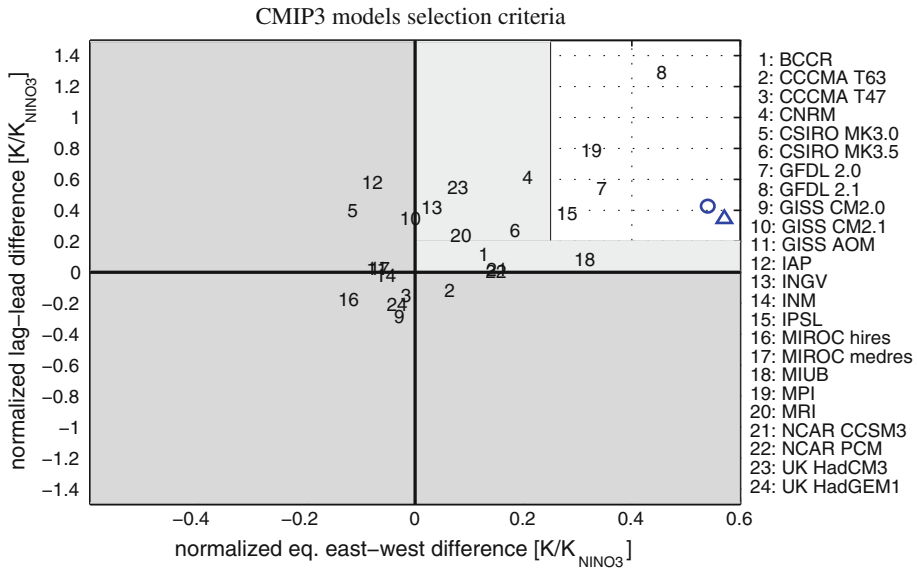

Fig. 8 CMIP3 models selection criteria Δ_{eq} and Δ_{time} for two different observational data sets (*circle* for HADISST and *triangle* for ERSST) and for the 24 CMIP3 models. The *shaded regions* are considered to be different from observations

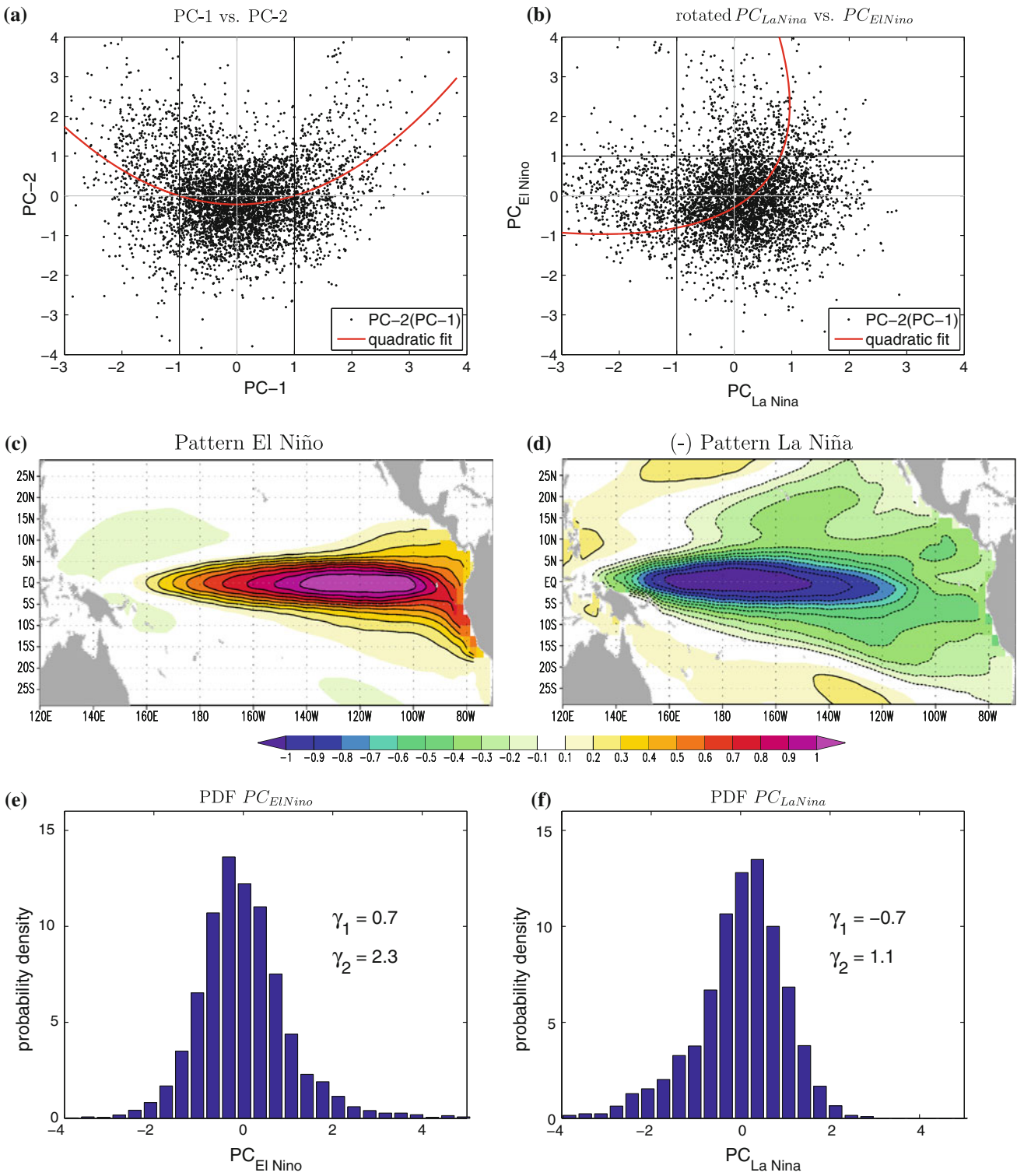

Fig. 9 Scatter plots, rotated patterns and the probability density functions of tropical Pacific SST PC-1 and PC-2 data pairs as in Fig. 4, but for the combined data set of the 4 CMIP3 models that passed the selection criteria Δ_{eq} and Δ_{time}

some capability in simulating this characteristic. In the following we will focus the analysis on these 4 models. We therefore treat the 4 models as one data set: defining anomalies for each of the models individually relative to the 20th century simulations linear detrended climatological mean values and combining the anomalies of the 4

models to one data set. However, we analyzed each of the 4 models individually and found that the characteristics discussed below are significant in all models.

The two leading EOF-modes (not shown) of the combined data set are very similar to those observed (Fig. 1). In particular the EOF-2 mode has a very similar east to west dipole along the equator with the western pole extending to the northern (more pronounced) and southern (less pronounced) subtropics. The EOF-1 appears to be slightly more pronounced in the CMIP models (46 % explained variance) and the EOF-2 is significantly weaker, with explaining only 7 % (it was 10 % in the observations) of the total variance.

The differences in the strong El Niño versus La Niña composites (as defined in the analysis for Fig. 2, but not shown) are not as pronounced as in the observations (see distribution along the x-axis of Fig. 8) and are stronger in the western Pacific warm pool region and much weaker in the eastern equatorial and coastal cold tongue region. The differences also do project on the EOF-2 in each of the 4 models separately, but correlation values are significantly lower than observed (0.92) ranging from 0.21 (IPSL) to 0.64 (GFDL 2.1) and the combined ensemble data set has a correlation value of 0.6.

Analog to the observations we can take a closer look at the non-linear interaction between the PC-1 and PC-2, see Fig. 9a. The distribution is quite similar to the observed, with a similar significant non-linear relation between PC-1 and PC-2. For extreme values of PC-1 PC-2 tends to be positive and for PC-1 near zero PC-2 tends to be negative, which is consistent with the observations. Again the non-linear model of Eq. (1) describes this non-linearity relatively well (correlation of 0.3), but not as good as in the observations. Overall the set of 4 models remarkably reproduces the observed non-linear interaction between PC-1 and PC-2, which is a strong support for a dynamical cause for this relationship.

Again we can rotate the distribution of Fig. 9a by 45° counter clockwise, as for the observations in Fig. 4b, to better highlight the extreme El Niño and La Niña events (Fig. 9b). The following can be noted here:

- As in the observations the models find very strong non-normal distributions for both $PC_{El\text{-}Niño}$ and $PC_{La\text{-}Niña}$, which is illustrated by the skewness and kurtosis values shown (Fig. 9e–f).
- The $PC_{El\text{-}Niño}$ has a quite significant positive skewness, but an even more significant kurtosis, highlighting the much larger probability of extreme events than expected from a normal distribution.
- The $PC_{La\text{-}Niña}$ distribution has again a quite significant negative skewness, suggesting a strong non-linearity towards extreme La Niña events that is not reflected in any of the conventional large-scale indices of ENSO.
- The patterns associated with the $PC_{El\text{-}Niño}$ and $PC_{La\text{-}Niña}$ (Fig. 9c–d) show the same east to west shift along the equator as observed; again supporting the idea that strong El Niño events are further to the east and more confined to the equator, and strong La Niña events are further to the west and have a larger latitudinal extent.

Based on the rotated $PC_{El\text{-}Niño}$ and $PC_{La\text{-}Niña}$ we can define the mean time evolution of composites of strong El Niño and La Niña events in analog to the analysis of the observations (Fig. 6a–c). The model results shown in Fig. 10a–c are quite similar to those of the observations: again at lag zero we find the equatorial dipole, but as mentioned above more pronounced in the western part. Even more pronounced than in the observations we find that strong El Niño events are followed by La Niña events and strong La Niña events are preceded by El Niño events. This again indicates some asymmetry in the driving forcing of strong El Niño and La Niña events in these four models.

The asymmetry in the Bjerknes feedbacks in the four models is shown in Fig. 10d–i. As in the observations we find the asymmetries in the zonal wind response to SST anomalies and in the relationship between zonal wind and thermocline depth anomalies. The later is in particular more pronounced in the models and marks a very strong non-linearity in the feedbacks of strong El Niño and La Niña events.

In summary the set of four CMIP3 models finds non-linear dynamics between strong El Niño and La Niña events, that are very similar to those observed. This supports the observed findings and suggests that the main processes causing these non-linearities are simulated in those four models.

6 ENSO in a simplified model: the RECHOZ model

Simplified models of ENSO help to deconstruct the elements of the ENSO dynamics and therefore help to better understand the interactions. In the following we use the ENSO recharge oscillator model after Burgers et al. (2005) coupled to a fully complex atmospheric GCM from Frauen and Dommenget (2010) in a 500 years long simulation (here named RECHOZ). The RECHOZ model simplifies the ocean dynamics to a 2-dimensional linear interaction between NINO3 SST and equatorial Pacific mean thermocline depth anomalies. The SST pattern in the tropical Pacific is by construction the fixed pattern of the observed EOF-1. It thus has only one degree of freedom in the tropical Pacific SST and no spatial pattern asymmetry (e.g. east-to-west) of ENSO events can exist in

this model. The analysis of Frauen and Dommenget (2010) showed that the RECHOZ model, despite its simplicity, has realistic skewness and seasonality of ENSO and a realistic standard deviation and power spectrum in the NINO3 SST index. The fact that the ocean dynamics are linear, of very low order and without any spatial degrees of freedom simplifies all non-linearities that this model produces to non-linearities caused by the atmospheric heat fluxes and zonal wind stress. Therefore, the model helps to explore how the atmospheric non-linear feedbacks contribute to the ENSO pattern and evolution non-linearities.

Further, the model is coupled to a simple single column mixed layer ocean outside the tropical Pacific to allow for SST variability independent of ENSO and also in response to ENSO dynamics. We will analyze an additional 500 years sensitivity experiment, in which we set the SST in the tropical Indian and Atlantic Oceans to climatology to explore the influence that SST forcing from outside the tropical Pacific may have on the ENSO non-linearity.

The simplicity of the model further allows us to compute a very large set of perfect model forecast ensembles. We therefore restarted the coupled model at the first of January at 100 different years, each start date 5 years apart from each other. For each restart we computed a set of four ensemble members for a 12 months long forecast, with each member starting from slightly perturbed initial SST conditions.

First, we take a look at the non-linearity in the time evolution of ENSO events in the RECHOZ control simulation. The time evolutions of strong El Niño and La Niña events in the RECHOZ model are shown in Fig. 11a–c. Since the pattern of ENSO events in the RECHOZ model is by construction fixed, the difference in the SST composites is by construction zero along the equator at lag zero. So by construction no east-to-west asymmetry of ENSO events can exist in this model. The only non-linearity in the SST that could exist in the RECHOZ model is in the time evolution of the events. Indeed we can see that some significant non-linearity between the time evolution of strong El Niño and La Niña events exist: As in the observations a strong El Niño event is followed by a La Niña event about 1 year later and a strong La Niña event is preceded by an El Niño event. Since the RECHOZ model has by construction no non-linearities in the ocean dynamics, the results suggest that the asymmetric time evolution of the strong ENSO events is at least partially caused by non-linearities in the atmospheric forcings.

The SLP anomalies per unit SST NINO3 anomaly in the strong El Niño events (not shown) are much stronger than those of the strong La Niña events, which is in the overall tendency similar to the observations (Fig. 7a–c). The zonal wind evolution shows a similar non-linearity between strong El Niño and La Niña events. Since the SST pattern is by construction always the same in the RECHOZ model, we can from this shift in the zonal winds clearly conclude that the atmosphere responds to the positive SST pattern more strongly and more shifted to the east. Following the studies of Zhang and McPhaden (2006, 2010), the shifted wind response would support the non-linearity in the observed SST patterns. Frauen and Dommenget (2010) further showed that this non-linearity in the zonal wind response is indeed sufficient to explain the skewness of ENSO in the RECHOZ model and is of similar strength than that observed.

The thermocline depth in the RECHOZ model is just one scalar number for the whole of the equatorial Pacific. Subsequently, the RECHOZ model equivalent analysis to the observed (Fig. 7g–h) or CMIP model (Fig. 10g–h) thermocline depth evolution during strong events is not a Hoevmoeller diagram, but is just the equatorial mean thermocline depth evolution as function of different lead times, see Fig. 12a–b. Again, we find the same asymmetry in the RECHOZ model as in the observations: strong La Niña events have a much more pronounced thermocline depth anomaly preceding the event, whereas strong El Niño events develop a strong negative thermocline depth anomaly after the event leading to the following La Niña conditions.

Frauen and Dommenget (2010) found that the non-linear behavior in the RECHOZ model can essentially be reduced to the non-linear response of the zonal wind stress to SST anomalies. They illustrated this by forcing the recharge oscillator equations with random white noise and by assuming a non-linear response of the zonal wind stress to SST anomalies (we refer to this model as REOSC-MC). The recharge oscillator equations of Frauen and Dommenget (2010) are two tendency equations, one for the NINO3 SST anomaly, T, and one for the mean equatorial thermocline depth anomaly, h, given by:

$$\frac{dT}{dt} = a_{11O}T + a_{12}h + c_{\tau A}\tau + \frac{1}{mc}f \tag{4}$$

$$\frac{dh}{dt} = a_{21O}T + a_{22}h + c_{\tau O}\tau \tag{5}$$

The forcings by the net atmospheric heat flux over the NINO3 region, f, and the zonal wind stress over the central Pacific region (160E–140W, 6S–6N), τ, are assumed to

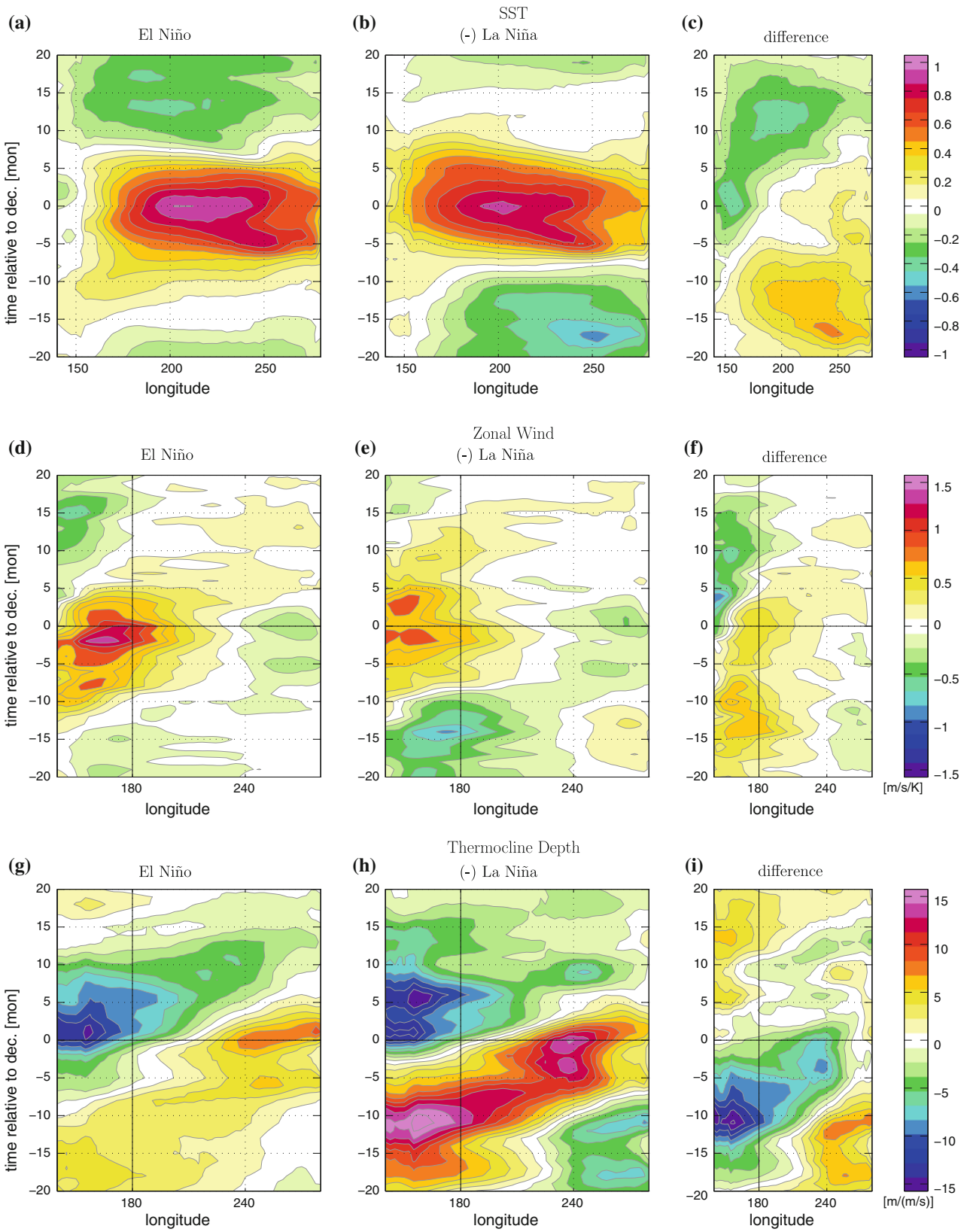

Fig. 10 Composite Hoevmoeller diagrams of the equatorial Pacific as in Fig. 6a–c, but for combined data set of the 4 CMIP3 models for **a–c** SST and **d–f** zonal wind and for **g–i** thermocline depth. The thermocline depth composites are normalized by the mean zonal wind anomalies in the central Pacific (160°E–120°W) and not by the NINO3.4 SST anomalies

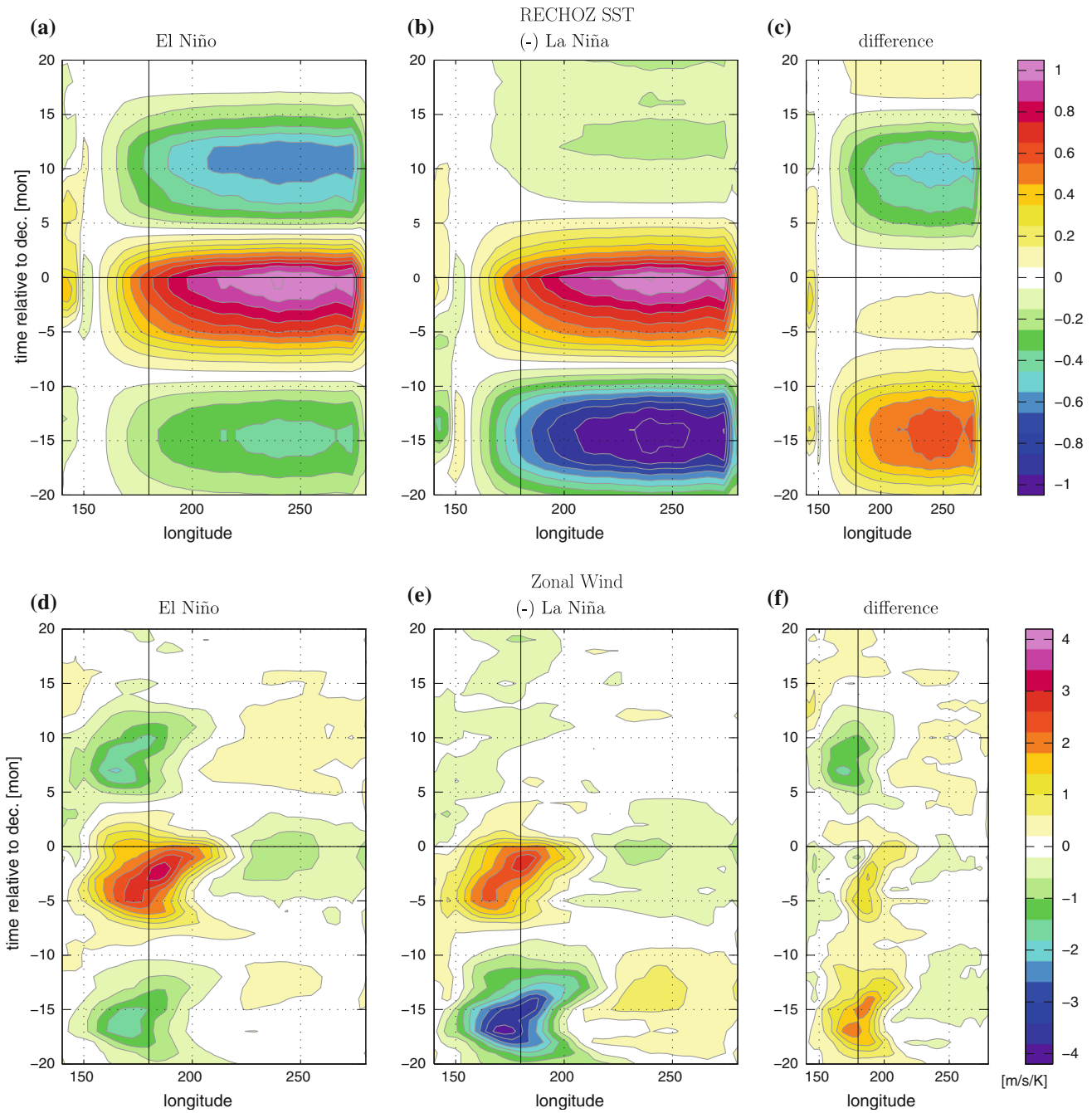

Fig. 11 Composite Hoevmoeller diagrams of the equatorial Pacific as in Fig. 6a–c but for the RECHOZ model **a–c** SST anomalies and **d–f** zonal wind anomalies. As a selection criteria the NINO3.4 SST is used instead of the $PC_{El\text{-}Niño}$ and $PC_{La\text{-}Niña}$ as no such corresponding non-linear PCs exist in the RECHOZ model

have one component that is a simple relationship to T and the remaining components are random noise forcings, ξ_1 and ξ_2:

$$f = r_{Tf}T + \xi_1 \tag{6}$$

For τ they assumed either a linear or quadratic relationship:

$$\tau = r_{T\tau}T + \xi_2 \tag{7}$$

$$\tau = r_{T\tau 1}T^2 + r_{T\tau 2}T + \xi_2 \tag{8}$$

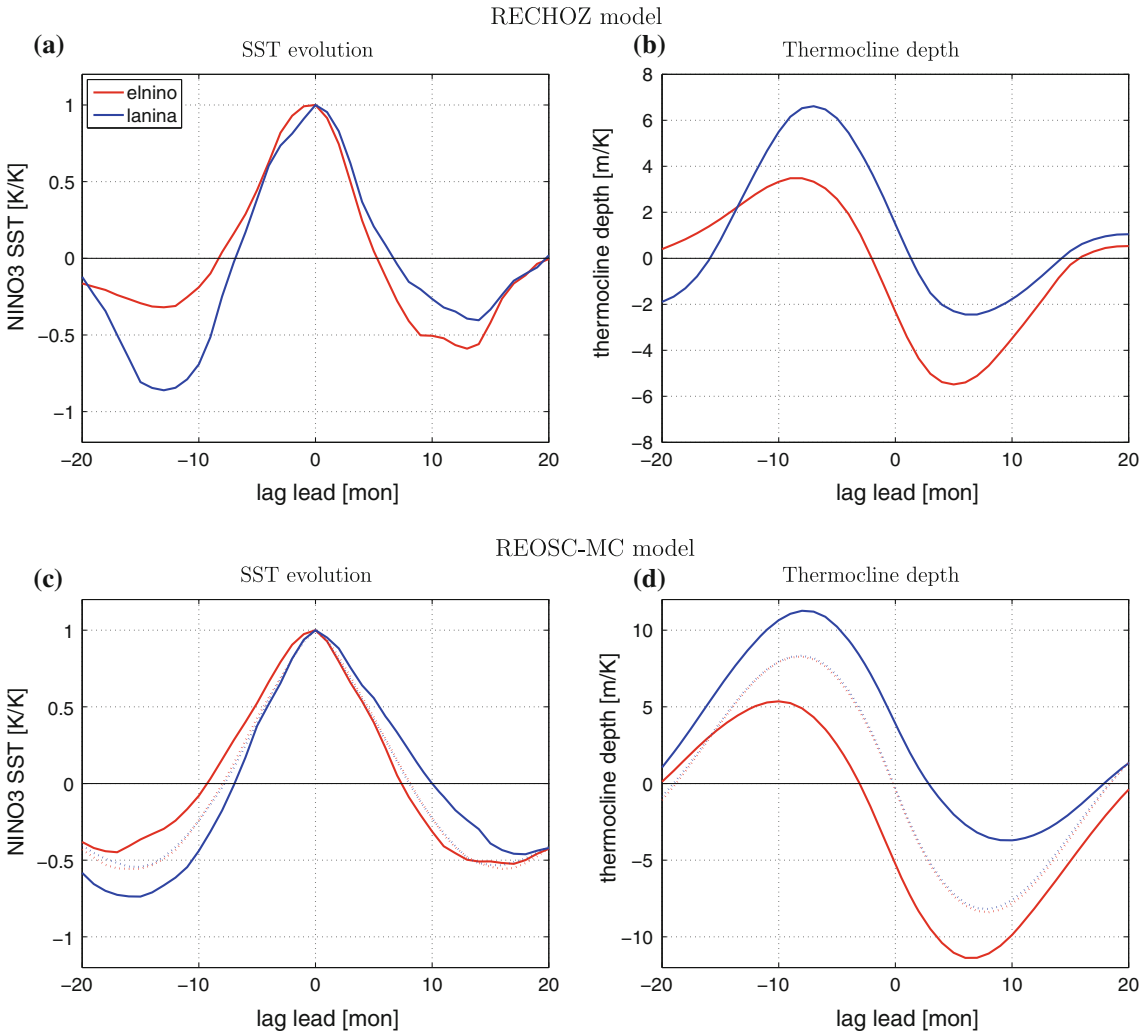

Fig. 12 Lag-lead composites of strong El Niño and La Niña events defined as in Fig. 11 for **a** NINO3 SST anomalies and **b** equatorial mean thermocline depth anomalies of the RECHOZ simulation. **c** and **d** as in (**a**) and (**b**), but for the linear (*dotted lines*) and non-linear (*solid lines*) REOSC-MC model

All parameters[1] of the REOSC-MC model were estimated from observations or model simulations, see Frauen and Dommenget (2010) for details. If this model is integrated with the linear relation between SST and zonal wind [Eqs. (4–7)] we get a linear model with no asymmetries, see Fig. 12c–d. However, if the REOSC-MC model assumes the quadratic relationship [Eq. (8)], than we basically reproduce the non-linear time evolution between strong El Niño and strong La Niña events in the RECHOZ model, see Fig. 12. Thus the non-linear time evolution in the RECHOZ model can be simplified to a non-linear response of the zonal wind stress to NINO3 SST anomalies.

In the analysis so far we noted that strong La Niña events have more pronounced ocean state anomalies and less pronounced atmospheric anomalies preceding the peak phase, indicating that they may be more forced by the ocean. In turn strong El Niño events appear to be more atmospherically forced. Since the ocean state is in general more persistent and therefor more predictable than the atmospheric state, it seems reasonable to assume that strong La Niña events may be better predictable than strong El Niño events.

We can test this idea with the large set of forecasts in the RECHOZ model simulations. In Fig. 13 we see the anomaly correlation skills for the NINO3 SST anomalies up to a forecast lead-time of 12 months for forecasts

[1] $a_{11O} = -0.62 \frac{1}{\text{month}}$, $a_{12} = 0.023 \frac{K}{\text{month}_m}$, $c_{\tau A} - 6.2 \times 10^{-12} \frac{Km\text{month}}{\text{kg}}$, $mc = 2.2 \times 10^{21} \frac{\text{kg}}{\text{month}^2 K}$, $a_{21O} = -0.84 \frac{m}{K\,\text{month}}$, $a_{22} = -0.021 \frac{1}{\text{month}}$, $c_{\tau O} - 2.9 \times 10^{-12} \frac{m^2\,\text{month}}{\text{kg}}$, $r_{Tf} = -1.4 \times 10^{20} \frac{\text{kg}}{\text{month}^3 K}$, $r_{T\tau} = 1.0 \times 10^{11} \frac{\text{kg}}{m\,\text{month}^2 K}$, $r_{T\tau 1} = 8.1 \times 10^{9} \frac{\text{kg}}{m\,\text{month}^2 K}$, $r_{T\tau 2} = 9.9 \times 10^{10} \frac{\text{kg}}{m\,\text{month}^2 K}$.

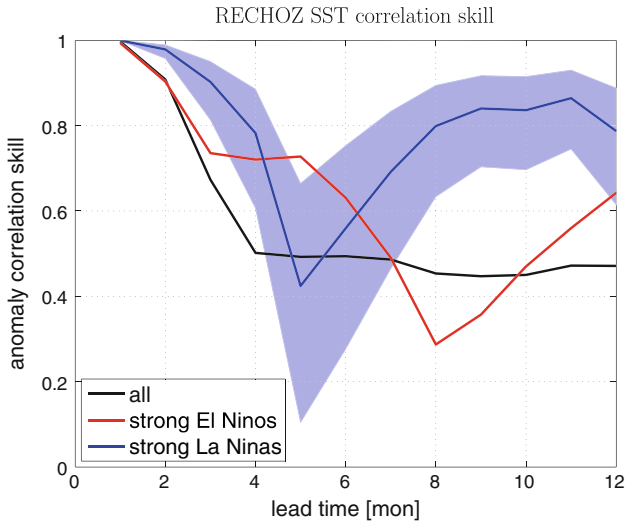

Fig. 13 Anomaly correlation skills for RECHOZ perfect model forecast ensembles. The strong El Niño/La Niña (*red/blue*) anomaly correlation skills are based on those forecasts ensembles that have an NINO3 SST anomaly >1.0/<−1.0 at 12 month lead-time in the RECHOZ control simulation. The *blue shaded area* marks the 90 % confidence interval for the La Niña forecasts

starting at the first of January. First of all we can note that the anomaly correlation skill of all 100 forecasts drops relatively sharply in April due to the spring predictability barrier. We created two subsets of forecast ensembles to highlight the differences in predictability for strong El Niño and La Niña events. We selected all those forecasts in which the control NINO3 SST anomaly at lead times of 12 months after the start date of the forecast (December) is larger than one standard deviation (strong El Niños) and smaller than minus one standard deviation (strong La Niñas). The anomaly correlation skill of the strong La Niña event forecasts is clearly larger than the one of the strong El Niños, illustrating that strong La Niña events at lead time of 12 months are much more predictable in the RECHOZ model than strong El Niño events.

ENSO events influence remote regions, such as the tropical Indian or Atlantic Oceans. In turn the tropical Indian Ocean and Atlantic Ocean provide a feedback onto the ENSO dynamics. It seems reasonable to assume that such feedbacks may contribute to the non-linear dynamics of ENSO. In particular Ohba and Watanabe (2012) argue that the asymmetric time evolution of ENSO events is at least partially caused by the interaction with the Indian Ocean. To estimate such feedbacks from the tropical Indian Ocean and Atlantic Ocean we can repeat the above analysis (Fig. 11) in the sensitivity experiment where the tropical Indian and Atlantic Oceans SST variability is decoupled (fixed to climatological values), see Fig. 14. We refer to this simulation as RECHOZ-PACO.

First of all we can note in Fig. 14a and b that the events last longer. This is in agreement with similar studies that also find that the coupling of the Indian and/or Atlantic Ocean leads to shorter period in ENSO variability and also to a damping of the variability (e.g. Kang and Kug 2002; Dommenget et al. 2006; Jansen et al. 2009; Frauen and Dommenget 2012). In the RECHOZ-PACO simulation the decoupling of the tropical Indian and Atlantic Oceans shifts the period of ENSO from about 3 years to about 4 years and increases the NINO3 SST standard deviation by about 60 %. However, more important for this study is the asymmetry in the evolution of strong El Niño versus strong La Niña events. This aspect is essentially unchanged (compare Fig. 11c with Fig. 14c), indicating that the non-linear evolution of the ENSO events is to first order not affected by the coupling to the other tropical oceans in the RECHOZ model. This apparent mismatch to the finding Ohba and Watanabe (2012) may be related to the fact that the RECHOZ model does not allow for changes in spatial pattern of ENSO events, which may indeed be important to explain the different sensitivities to the Indian Ocean feedbacks.

7 El Niño Modoki

In recent years several publications have argued for different types of El Niño events, calling them Central Pacific or Modoki El Niño (e.g. Ashok et al. 2007 or Kao and Yu 2009). The authors basically argue that these different types of ENSO events happen independent of each other (unrelated) and would be controlled by different kind of dynamics. The definition of these El Niño types is projecting on both EOF-1 and EOF-2 and therefore overlaps with definitions of the rotated $PC_{El\text{-}Niño}$ and $PC_{La\text{-}Niña}$ introduced in this study. It is therefore instructive to discuss how these definitions of ENSO types relate to the present analysis. A similar discussion is also given in Takahashi et al. (2011). A few points should be noted here to put the Central Pacific or Modoki El Niño type of definitions into the perspective on the non-linearity of ENSO:

- Ashok et al. (2007) motivated the definition of the El Niño Modoki on the basis of the EOF-2. They argue that since the eigenvalue of EOF-2 is statistically well separated from the other eigenvalues it can be considered as a mode of variability independent from EOF-1. This simplistic interpretation of EOF modes is indeed problematic, as discussed in Dommenget and Latif (2002). Individual EOF modes cannot be discussed independently of the other EOF modes, we have to consider that the SST variability is a high dimensional multivariate stochastic process and the EOF modes are

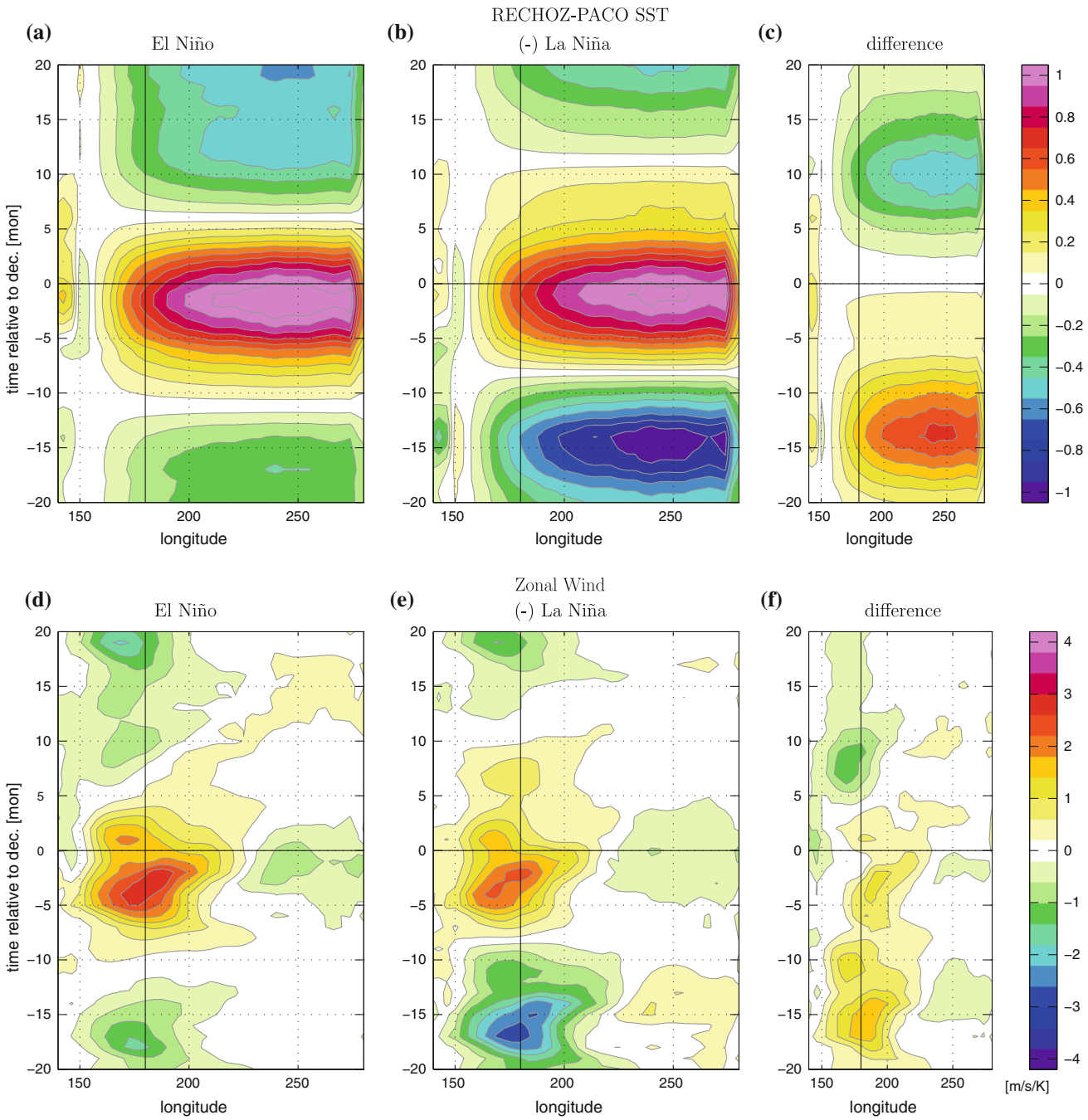

Fig. 14 Composite Hoevmoeller diagrams of the equatorial Pacific as in Fig. 11 but for the RECHOZ-PACO simulation

a representation of it, see Dommenget (2007) for a discussion. In Sect. 3 we have demonstrated that a significant fraction (26 % of the total variance) of EOF-2 can be linked to the variability of EOF-1. However, it needs to be noted that the largest fraction of EOF-2 is unrelated to this relationship. This means that a significant part of the variations in the pattern of ENSO events remains. Whether these variations are purely random, following, for instance, a spatial red noise process as described in Dommenget (2007), or are linked to another low-order mode of variability is unclear from the analysis present here, in Ashok et al. (2007) or in Kao and Yu (2009).

- The definition of El Niño Modoki or central Pacific El Niños is roughly identical to the $PC_{La\text{-}Niña}$. It thus strongly projects on the La Niña pattern. Since the distribution of $PC_{La\text{-}Niña}$ is strongly negatively skewed, extreme positive events are essentially not observed.

Thus El Niño Modoki or central Pacific El Niños events will always fall into the category of weak El Niño events. Modoki or central Pacific El Niños are unlikely to be strong events. Since the $PC_{La\text{-}Niña}$ (El Niño Modoki) distribution is dominated by the extreme negative events (La Niñas) and not by positive events (El Niño Modoki), linear regression analysis based on El Niño Modoki or central Pacific El Niños indices (roughly $PC_{La\text{-}Niña}$) is essentially an analysis of La Niña events but with the sign reversed.

- If we simplify ENSO to one fixed pattern (EOF-1), we can roughly describe it by a linear (normally distributed) behavior (see Fig. 1c). In contrast, if we focus on spatial variations of the ENSO patterns, such as the El Niño Modoki, central Pacific El Niño indices (roughly $PC_{La\text{-}Niña}$) or the discussion we have presented in the above analysis, then non-linearities (non-normal distribution) become dominant (as illustrated by Figs. 2, 4 or 5) and are indeed central to the understanding of the dynamics.
- Most CMIP3 models are quite bad in simulating the non-linearities of ENSO, in particular the pattern and time evolution non-linearities. Subsequently, analyses of the CMIP3 models El Niño Modoki or central Pacific El Niño indices for present or future climate change are quit limited in skill, as it is very unclear whether or not the bulk of the models in the CMIP3 database are capable of simulating the appropriate non-linear dynamics of the El Niño Modoki or central Pacific El Niño indices.

8 Summary and discussion

In this study we analyzed the observed non-linearity in the ENSO SST pattern and time evolution. Some of the observational findings were only marginally significant, but were backed up with additional support from state of the art CGCM simulations. Some insight into the feedbacks causing the observed non-linearities were based on observational evidence and state of the art CGCM simulations, but most insight were gained by the analysis of the strongly simplified hybrid coupled RECHOZ model of Frauen and Dommenget (2010). The main findings of this study can be summarized and discussed by the following points:

- The observed ENSO events have some significant non-linearity in their spatial SST pattern between positive (El Niño) versus negative (La Niña) and strong versus weak events. Strong El Niño events are shifted to the east and are more closely confined to the equator than strong La Niña events, which are more shifted to the central equatorial Pacific and are wider in their meridional extend. The opposite holds for weak El Niño events, which are more shifted to the central equatorial Pacific and are wide in their meridional extend, whereas weak La Niña events are more like strong El Niño events with opposite signs and weaker. Thus they are more easterly and more confined to the equator. In turn East Pacific ENSO events are mostly strong El Niño and weak La Niña events while Central Pacific events are mostly strong La Niña and weak El Niño events.
- This has important implications for the teleconnections of ENSO events, which are likely to follow some of these non-linearities. Here it has to be noted that most studies analyze the impact of ENSO events in a canonical way, assuming a linear relation between positive versus negative and strong versus weak events. Thus they describe ENSO by one impact pattern. However, ENSO impact studies should distinguish between the positive versus negative and strong versus weak categories and describe the impact of ENSO according to the four categories, if the database allows for such differentiations.
- This spatial non-linearity of ENSO events can be modeled relatively well by a non-linear (quadratic) relationship between PC-1 and PC-2. It was illustrated that the residual SST variability has very little spatial non-linearity of ENSO events left (see Fig. 5).
- The analysis of the non-linear (quadratic) relationship between PC-1 and PC-2 suggest that a 45° rotation of the EOF-1 and EOF-2 modes into the two rotated modes $PC_{El\text{-}Niño}$ and $PC_{La\text{-}Niña}$ would be a better presentation of extreme El Niño and La Niña events. The $PC_{El\text{-}Niño}$ mode represents a mode that most strongly projects onto strong El Niño events and has a pattern matching those of strong El Niño events, with large amplitudes in the eastern Pacific and mostly confined to the equator. The pattern of the $PC_{La\text{-}Niña}$ mode is very similar to the pattern of extreme La Niña events with opposite sign, showing a central Pacific peak and a wide meridional extend.
- The probability distribution of $PC_{El\text{-}Niño}$ has a very strong positive skewness and kurtosis, highlighting the strong tendency to have positive extreme events. This is consistent with previous studies illustrating that the positive skewness in SST is stronger in the eastern Pacific and also in index regions closer to the east (e.g. NINO1 region), see Burgers and Stephenson (1999).
- More interestingly we find that the $PC_{La\text{-}Niña}$ mode probability distribution has a very strong negative skewness, highlighting the strong tendency to have negative (La Niña) extreme events. This is not reflected in any of the large-scale indices of ENSO (e.g. EOFs, NINO1, 2, 3 or 4 regions), but seems to be consistent

with the tendency for regional SST variability to be more negatively skewed in the western equatorial Pacific (Burgers and Stephenson 1999). Thus, we find two strongly skewed modes of variability in the equatorial Pacific: One in the east (El Niño) tending towards strong positive events and one in the central Pacific (La Niña) tending towards strong negative events.

- The time evolution of observed strong El Niño and La Niña events revealed an indication of another asymmetry in the build up and decay of strong events: The La Niña events that follow a strong El Niño events tend to be stronger than those preceding. In contrast no El Niño events follow after strong La Niña events, but significant El Niño events are preceding strong La Niña events. This finding is consistent with previous studies that describe that La Nina events tend to last longer (e. g. Okumura and Deser 2010). This asymmetry in the evolution of events is indicating an asymmetry in the driving mechanisms of the events and therefore a non-linearity in the feedbacks controlling the events.
- The combined analysis of observations, state of the art coupled climate models and most importantly the simplified RECHOZ model suggests that the non-linear response in the zonal wind in the central Pacific to SST anomalies is important to understand both the east-west shift of events and the asymmetry in the time evolution of events. The zonal winds response to positive SST anomalies is stronger and further to the east than for negative SST anomalies, as it has also been shown in observations by Kang and Kug (2002) and in the RECHOZ model by Frauen and Dommenget (2010). The shift to the east in the zonal wind response is likely to cause the SST response to be also shifted to the east (e.g. Zhang and McPhaden 2006, 2010), explaining the eastward shift of strong El Niño events. The stronger amplitude in the zonal wind response during strong El Niño events leads to a stronger build up of a negative thermocline depth anomaly, which sets the ocean state for the decay of the El Niño event and the development of the following La Niña event about a year later.
- This non-linearity in the strength of the zonal wind response leads to an overall asymmetry in the thermocline depth anomalies preceding strong El Niño and strong La Niña events. Based on the simplified RECHOZ model we could demonstrate that the much more pronounced thermocline depth anomalies preceding strong La Niña events make those events more predictable than strong El Niño events. In turn, we can conclude that strong El Niño events are more likely to be forced by atmospheric fluctuation and are therefore less predictable.
- The generally known non-linearity of the amplitude of ENSO events (e.g. stronger El Niños than La Niñas) can thus be understood to be also linked to an ENSO non-linearity in the pattern and time evolution by the stronger and further eastward sensitivity of zonal winds in the central Pacific to positive SST anomalies than to negative SST anomalies.
- While there is a set of 4 CMIP3 models that strongly support the above described non-linearity in the pattern and time evolution of ENSO events a large number of state of the art coupled models is not capable of simulating these non-linearities in the ENSO mode realistically. Thus, this non-linear behavior of ENSO marks a significant deficiency in many current state of the art coupled models and results on the ENSO pattern variation or asymmetry in their time evolution using the entire CMIP3 ensemble should be taken with care.
- Finally, we need to note that we linked the non-linearities in the ENSO mode only to non-linearities in the zonal wind response to SST anomalies. This does not indicate in any way that other non-linear processes in the atmosphere or ocean do not contribute to this phenomenon in a significant way. The fact that we only discussed the zonal wind non-linearity is merely reflecting the limited amount of observations and simulations that we had available for this analysis.

Acknowledgments We like to thank Harry Hendon, Neville Nicholls and Yuko Okumura for fruitful discussions and comments. We also like to thank two anonymous referees for their comments. This study was supported by the ARC Centre of Excellence in Climate System Science (CE110001028), the ARC project "Beyond the linear dynamics of the El Nino Southern Oscillation" (DP120101442) and the Deutsche Forschung Gemeinschaft (DO1038/5-1).

References

An SI, Ham YG, Kug JS, Jin FF, Kang IS (2005) El Nino La Nina asymmetry in the coupled model intercomparison project simulations. J Clim 18:2617–2627

Ashok K, Behera SK, Rao SA, Weng HY, Yamagata T (2007) El Nino Modoki and its possible teleconnection. J Geophys Res Oceans 112

Burgers G, Stephenson DB (1999) The "normality" of El Nino. Geophys Res Lett 26:1027–1030

Burgers G, Jin FF, van Oldenborgh GJ (2005) The simplest ENSO recharge oscillator. Geophys Res Lett 32

Carton JA, Chepurin G, Cao XH (2000) A simple ocean data assimilation analysis of the global upper ocean 1950–95. Part II: results. J Phys Oceanogr 30:311–326

Choi J, An S-I, Yeh S-W (2012) Decadal amplitude modulation of two types of ENSO and its relationship with the mean state. Clim Dyn 38:2631–2644. doi:10.1007/s00382-011-1186-y

Dommenget D (2007) Evaluating EOF modes against a stochastic null hypothesis. Clim Dyn 28:517–531

Dommenget D, Latif M (2002) A cautionary note on the interpretation of EOFs. J Clim 15:216–225

Dommenget D, Semenov V, Latif M (2006) Impacts of the tropical Indian and Atlantic Oceans on ENSO. Geophys Res Lett 33

Frauen C, Dommenget D (2010) El Nino and La Nina amplitude asymmetry caused by atmospheric feedbacks. Geophys Res Lett 37

Frauen C, Dommenget D (2012) Influences of the tropical Indian and Atlantic Oceans on the predictability of ENSO. Geophys Res Lett 39

Hoerling MP, Kumar A, Zhong M (1997) El Nino, La Nina, and the nonlinearity of their teleconnections. J Clim 10:1769–1786

Jansen MF, Dommenget D, Keenlyside N (2009) Tropical atmosphere-ocean interactions in a conceptual framework. J Clim 22:550–567

Kalnay E, Kanamitsu M, Kistler R, Collins W, Deaven D, Gandin L, Iredell M, Saha S, White G, Woollen J, Zhu Y, Chelliah M, Ebisuzaki W, Higgins W, Janowiak J, Mo KC, Ropelewski C, Wang J, Leetmaa A, Reynolds R, Jenne R, Joseph D (1996) The NCEP/NCAR 40-year reanalysis project. Bull Am Meteorol Soc 77:437–471

Kang IS, Kug JS (2002) El Nino and La Nina sea surface temperature anomalies: asymmetry characteristics associated with their wind stress anomalies. J Geophys Res Atmos 107

Kao HY, Yu JY (2009) Contrasting eastern-pacific and central-pacific types of ENSO. J Clim 22:615–632

Keenlyside NS, Latif M (2007) Understanding equatorial Atlantic interannual variability. J Clim 20:131–142

Larkin NK, Harrison DE (2002) ENSO warm (El Nino) and cold (La Nina) event life cycles: ocean surface anomaly patterns, their symmetries, asymmetries, and implications. J Clim 15:1118–1140

Larkin NK, Harrison DE (2005) Global seasonal temperature and precipitation anomalies during El Nino autumn and winter. Geophys Res Lett 32

Marsland SJ, Haak H, Jungclaus JH, Latif M, Roske F (2003) The Max-Planck-Institute global ocean/sea ice model with orthogonal curvilinear coordinates. Ocean Model 5:91–127

McPhaden MJ, Lee T, McClurg D (2011) El Nino and its relationship to changing background conditions in the tropical Pacific Ocean. Geophys Res Lett 38

Meehl GA, Covey C, Delworth T, Latif M, McAvaney B, Mitchell JFB, Stouffer RJ, Taylor KE (2007) The WCRP CMIP3 multimodel dataset—a new era in climate change research. Bull Am Meteorol Soc 88:1383–+

Monahan AH (2001) Nonlinear principal component analysis: tropical Indo-Pacific sea surface temperature and sea level pressure. J Clim 14:219–233

Ohba M, Ueda H (2009) Role of nonlinear atmospheric response to SST on the asymmetric transition process of ENSO. J Clim 22:177–192

Ohba M, Watanabe M (2012) Role of the Indo-Pacific interbasin coupling in predicting asymmetric ENSO transition and duration. J Clim 25

Ohba M, Nohara D, Ueda H (2010) Simulation of asymmetric ENSO transition in WCRP CMIP3 multimodel experiments. J Clim 23:6051–6067

Okumura YM, Deser C (2010) Asymmetry in the duration of El Nino and La Nina. J Clim 23:5826–5843

Philip S, van Oldenborgh GJ (2009) Significant atmospheric nonlinearities in the ENSO cycle. J Clim 22:4014–4028

Rayner NA, Parker DE, Horton EB, Folland CK, Alexander LV, Rowell DP, Kent EC, Kaplan A (2003) Global analyses of sea surface temperature, sea ice, and night marine air temperature since the late nineteenth century. J Geophys Res Atmos 108

Rodgers KB, Friederichs P, Latif M (2004) Tropical pacific decadal variability and its relation to decadal modulations of ENSO. J Clim 17:3761–3774

Schopf PS, Burgman RJ (2006) A simple mechanism for ENSO residuals and asymmetry. J Clim 19:3167–3179

Smith TM, Reynolds RW, Peterson TC, Lawrimore J (2008) Improvements to NOAA's historical merged land-ocean surface temperature analysis (1880–2006). J Clim 21:2283–2296

Sun FP, Yu JY (2009) A 10–15-years modulation cycle of ENSO intensity. J Clim 22:1718–1735

Takahashi K, Montecinos A, Goubanova K, Dewitte B (2011) ENSO regimes: reinterpreting the canonical and Modoki El Nino. Geophys Res Lett 38

van Oldenborgh GJ, Philip SY, Collins M (2005) El Nino in a changing climate: a multi-model study. Ocean Sci 1:81–95

Yeh SW, Kug JS, Dewitte B, Kwon MH, Kirtman BP, Jin FF (2009) El Nino in a changing climate. Nature 461:511–514

Yu JY, Kim ST (2011) Reversed spatial asymmetries between El Nino and La Nina and their linkage to decadal ENSO modulation in CMIP3 models. J Clim 24:5423–5434

Zhang XB, McPhaden MJ (2006) Wind stress variations and interannual sea surface temperature anomalies in the eastern equatorial Pacific. J Clim 19:226–241

Zhang XB, McPhaden MJ (2010) Surface layer heat balance in the eastern equatorial Pacific Ocean on interannual time scales: influence of local versus remote wind forcing. J Clim 23: 4375–4394